

Response to the Comments of the Executive Editor

Dear authors,

I would like to highlight a couple of issues related to compliance with our code availability policy. The main problem here is that the ISORROPIA II v2.3 and ISORROPIA-lite v1.0 codes are stored in a repository that we can not accept. You must store them in one of the repositories that we can accept, which are listed in our policy.

Also, although we are aware of the licensing issues with MESSY, we would like to ask you to store its code in a Zenodo private repository. In this way, you continue having control of its distribution, and at the same time, they are assured the long-term archival and the availability of a DOI to cite it.

Then, please, reply to this comment with the DOI and links for the new repositories, and remember to add this information to any newly reviewed version of your manuscript.

Following the advice of the Executive Editor and in order to comply with both the GMD policy and the MESSy license restrictions, we have stored our code, including the ISORROPIA versions used in our study, in a Zenodo private repository. We would like to emphasize that the ISORROPIA thermodynamic equilibrium model was used in our study only as part of the MESSy system and not as a stand-alone box model. The section on code availability was revised as follows: “The code developed in this study and all relevant features, including the ISORROPIA II v2.3 and ISORROPIA-lite v1.0 thermodynamic equilibrium codes as part of the MESSy system, are archived with a restricted access DOI (<https://doi.org/10.5281/zenodo.8379120>) and have already been incorporated into the official development branch of the EMAC modelling system and will therefore be part of all future released versions.”

Authors' Response to Anonymous Referee's #1 Comments:

Summary

This study presents the results from the EMAC simulations when different versions of the coupled ISORROPIA thermodynamic modules are used. The study is focused on the main inorganic aerosols (i.e., SO_4^{2-} , NO_3^- , and NH_4^+), together with changes in the aerosol water and acidity. The authors conclude that the new version of ISORROPIA (i.e., ISORROPIA-lite) is computationally more efficient than the previous versions of the thermodynamic module (i.e., ISORROPIA II v1 and v2.3, both for stable and metastable modes) and is therefore a good replacement for 3D global simulations. The paper is well-written and well-organized, and the conclusions are useful in exploring the uncertainties of using different versions and setups of the ISORROPIA thermodynamic module in global models. However, the authors can address a few minor issues before the final publication in GMD to make the proposed parameterizations easier to understand for the reader.

We would like to thank the reviewer for his/her thoughtful review and positive response. Below is a point-by-point response (in black) to the comments and suggestions (in blue)

General Comments

- 1. The authors present the differences in simulating inorganic aerosols due to the various versions of the ISORROPIA thermodynamic module. Although the differences are minimal, the authors could provide some additional information on their findings. For example, the authors only state that the differences between ISORROPIA v1 and v2.3 are due to improvements in acidity calculations (Song et al. 2018), or the differences between ISORROPIA v2.3 and the lite version under the same conditions are, on average, less than 5%. Some additional sentences on the impact of these updates to the code on the simulated concentrations of inorganic aerosol components would be useful for the reader.*

We have followed the suggestion of the reviewer and added information about the differences between ISORROPIA II v1 and v2.3. We also mention that the interested reader can find additional details about these differences in Song et al. (2018). The updates in the code from ISORROPIA II v1 to v2.3 affected only a small number of the simulations in this work, in which the model failed to accurately consider the evaporation of NH_3 . In these few instances, the pH estimated by ISORROPIA v1 was unrealistically close to neutrality. However, because this was quite rare these problems had a minimal effect on the average predicted levels of gas phase NH_3 and aerosol concentrations.

- 2. Considering that the gas-particle partitioning of semi-volatile species such as HNO_3 is very sensitive to the calculated acidity levels and aerosol water concentrations, the authors could discuss more about why these differences exist in the model among the different versions of ISORROPIA, providing additional global maps for the main inorganics and focusing particularly on regions where such differences (positive or negative) are important. This, along with a slightly more detailed technical description of the advances in thermodynamic*

calculations and the evolution of the ISORROPIA module, will help the reader understand and interpret the presented sensitivity simulations.

Since the largest discrepancies between the various ISORROPIA versions are observed for nitrate, appropriate regions have been selected and further analyzed to investigate the source of these differences. These regions were chosen because they have high nitrate concentrations, but also because the predictions of the various ISORROPIA versions for aerosol water and acidity differ significantly over these areas. Therefore, this analysis covers the regions with high sensitivity to HNO₃ partitioning at least as far as ISORROPIA is concerned. A sentence clarifying this has been added towards the end of Section 4.1 of the revised manuscript. More information is also provided in Section 1 regarding the historical development of the thermodynamic calculation procedures during the evolution of ISORROPIA. Finally, Section 2.2 has been revised to include more details on the transition from ISORROPIA II to ISORROPIA-lite and the differences between the two modules.

- 3. Finally, the authors present a comparison of EMAC simulations between ISORROPIA-lite and ISORROPIA II in stable mode. It is not clear why such a comparison is shown here, especially taking into account previous works of the authors. Is it because these are the standard versions available now in the EMAC model? If the "comparison is done in an attempt to quantify the effects of using the metastable case in global atmospheric simulations," as stated in the manuscript, why didn't the authors just use the metastable mode of ISORROPIA II v2.3 to show that? Wouldn't a fair comparison between the two versions require them to be in the same (metastable) mode? Further discussion is needed to support this choice since the results of the different ISORROPIA aerosol modes (i.e., stable vs. metastable) are, indeed, expected to differ.*

Indeed, it is expected that results will differ when using different ISORROPIA versions with different aerosol state assumptions. However, it is our goal to determine under which conditions and over which regions these expected differences will occur and to what extent. The reason for this is that since ISORROPIA-lite will be available alongside ISORROPIA II (in stable mode) in the new EMAC model version, it would be useful for potential users to be informed about such differences and to choose the appropriate ISORROPIA version depending on the application and the desired efficiency and/or state assumption. Further discussion has been implemented in the revised manuscript in Sections 4.1 and 5.

Specific Comments

- 4. In Sect. 4.1 (p. 14), the authors present the differences in SO₄²⁻ annual mean surface concentrations between ISORROPIA-lite and ISORROPIA II (in stable mode). Does ISORROPIA II directly impact the SO₄²⁻ concentrations in the model, e.g., through the formation of insoluble CaSO₄ and its precipitation out of the aerosol aqueous phase? Does the model also consider sulfate production in aerosol water? Does the difference in inorganics from ISORROPIA calculations impact cloud acidity in the model and, thus, the respective sulfate production? Please discuss.*

ISORROPIA II has no direct impact on the predicted sulfate concentrations in the model since sulfuric acid is assumed to be practically non-volatile and to be present in the particulate phase, regardless of the state assumption used. However, differences in the predicted sulfate concentrations by EMAC in the versions using ISORROPIA-lite and ISORROPIA II in stable mode may result from indirect changes in wet deposition due to the different physical state of the aerosol. The formation of the CaSO_4 salt does not play a role in the predictions, since this specific salt is the only compound present in the solid state even in ISORROPIA-lite (more details can be found in Section 2.2. of the revised manuscript). Furthermore, the model does not account for sulfate production in aerosol water, but it does account for sulfate production in clouds via aqueous phase chemistry. Any differences between the two ISORROPIA versions in the inorganic aerosol ion balance (less than one pH unit) are not expected to have a significant effect on cloud acidity, which can also affect sulfate production. The higher water content in cloud droplets should smooth out any changes in aerosol acidity between the two versions, which in any case occur mostly in areas of very low RH and no cloud formation. More details about the expected differences in the predicted sulfate concentrations between the two model versions have been added to the appropriate part of Section 4.1.

5. In Sect. 4.1 (p. 14; l. 456), the authors state that the absolute differences between ISORROPIA-lite and ISORROPIA II for the fine NO_3^- are greater than those of coarse mode. Although this can be explained due to the different aerosol states used for ISORROPIA among the two simulations, it would be helpful to show which version of the thermodynamic model produces results that are closer to observed values. Can such a difference in the coarse aerosols also emerge through the assumption of kinetic limitations applied in the model during condensation of HNO_3 in the coarse mode? Although the parameterization is well documented in the literature, a somewhat more extended discussion would be useful for the reader.

The comparison of the ISORROPIA-lite results with observations was performed in order to evaluate the new model version and to establish that it is a reliable model for the calculation of inorganic aerosol composition. The ISORROPIA II thermodynamic module has been extensively validated against observations in previous studies (De Meij et al., 2012; Pozzer et al., 2012; Karydis et al., 2016; Metzger et al., 2018). However, following the reviewer's recommendation, we have performed a statistical analysis of the comparison between observations and ISORROPIA II predictions in stable mode, which is now included in the revised supplement. Although the two versions show similar performance, it should be emphasized that better performance on certain statistical metrics should not be taken as an indication that one state assumption is more scientifically valid than the other. A corresponding discussion has been added in Section 3.3. The evaluation results of ISORROPIA-lite and ISORROPIA II in the metastable are almost identical and this is now clearly stated in the revised manuscript. Regarding the kinetic limitations during the condensation of HNO_3 simulated in the model, the algorithm used is the same for both ISORROPIA versions and is applied before ISORROPIA calculates the gas/particle partitioning. The algorithm assumes that the amount of HNO_3 that can condense in each size mode within the model time step depends on the size of the aerosol and not on its physical state. The "metastable aerosol" is expected to be larger than a "stable aerosol" due to the potentially higher amount of water it contains, but this difference is small compared to the actual size of the aerosol mode (e.g., coarse vs. accumulation mode), especially for the coarse particles. This information has been added to Section 2.2, which describes the partitioning algorithm.

6. *In Sect. 4.3 (p. 23), the authors state that the pH values are calculated based on instantaneous H^+ and H_2O values estimated every 5 hours. Why specifically 5 hours? Does the model produce instantaneous outputs only every 5 hours by default (standard output), and that is the reason the authors use the most frequent model output? Does this, further, mean that a more frequent instantaneous output (e.g., hourly) would potentially produce more accurate pH results? Please discuss.*

The model user has the ability to control the frequency and the type (instantaneous or average values) of the output for most variables. The most commonly used, is the daily average output. However, Karydis et al. (2021) showed that a low temporal resolution output with average values can lead to a low biased calculated pH. This is due to Jensen's inequality (Jensen, 1906), which states that the convex transformation of an average value (e.g., the pH of the average H_2O and H^+ concentrations) is less than or equal to the average applied after the convex transformation (e.g., the average of all pHs calculated based on the instantaneous H_2O and H^+ values). For this reason, we chose to output the instantaneous values of H_2O and H^+ instead of the average. In addition, we chose to output every 5-hour interval to always get values at different times of the day and to account for the diurnal variability of pH (i.e., not possible with 6- or 8-hour intervals). The critical choice here is the instantaneous output (instead of averages), not the time resolution. Certainly, an hourly instantaneous output would provide more accurate pH estimates, but it will also increase the size of the data produced by a factor of five. More details on this choice have been added as further discussion in Section 4.3 of the revised manuscript.

7. *Karydis et al. (2021) showed that the metastable assumption produces more acidic particles in regions with high concentrations of mineral cations, such as downwind desert areas, and low RH values. As expected, almost the same results are presented here when comparing the ISORROPIA-lite (i.e., only in the metastable mode) and ISORROPIA II (in stable mode) simulations. It is not clear, thus, the added value of such a comparison here. Can you please discuss more?*

As this study presents the first results after the implementation of ISORROPIA-lite in the EMAC global model, this comparison was performed to assess whether this version can produce credible pH estimates on a global scale. This capability of ISORROPIA II is well established in the literature (e.g. Karydis et al., 2021). Therefore, in case EMAC users decide to use ISORROPIA-lite for aerosol composition simulations, we wanted to ensure that the aerosol pH estimates are reliable and indeed similar to the estimates of ISORROPIA II using the metastable assumption. Furthermore, it is important for the user to know the differences on the estimated pH values between the two available versions of the ISORROPIA module in the new EMAC model version. More details about the inclusion of this particular comparison and further discussion about it, have been added at the beginning of Section 4.3 as well as Section 5 of the revised manuscript.

8. *It is well established that NH_3 is the major buffer in most regions of the world. Therefore, if all NH_3 emissions were turned off, the thermodynamic system would definitely give unrealistic results, and as expected, aerosol particles would be extremely acidic. Maybe doubling or cutting in half NH_3 emissions would make more sense to explore potential differences in the responses on the two versions. It would also be advantageous to discuss the presence of non-*

volatile crustal species from sea salt and dust and how drastically they can change (increase) the aerosol pH in ISORROPIA-lite simulations compared to ISORROPIA v2.3 in the metastable mode. This would also give additional information on the impact of binary activity coefficient calculation between the two versions.

We agree with the reviewer that switching off all NH₃ emissions results in an unrealistic thermodynamic system that would lead to very acidic aerosols. This sensitivity simulation was only performed to verify that in some regions the presence of very high NH₃ concentrations can lead to such an increase in the pH of the fine aerosols that it can exceed the calculated alkalinity of the coarse particles. Following the reviewer's recommendation, we performed a sensitivity simulation in which the NH₃ emissions were reduced by half. The results are shown in Figure 10 of the revised manuscript. In addition, while the presence of non-volatile crustal species does indeed increase aerosol pH, Karydis et al. (2021) have shown that their role in regulating aerosol acidity is small compared to the buffering provided by NH₃ emissions.

9. *Sect. 3.3: It would be very useful to also present the seasonal variation for the comparison of the main inorganics (where available) between observations and model predictions, not only the annual mean values. Additionally, you can present the evaluation of the other sensitivity simulations performed for this study, not only the ISORROPIA-lite. This would help the reader better understand the pros and cons of each assumption.*

We have performed a seasonal statistical analysis to compare observations and predictions of both ISORROPIA-lite and ISORROPIA II in the stable state for the three main inorganic aerosol components, since these two model versions will be available to the user in the next release of the EMAC model. Since the predictions of ISORROPIA-lite were almost identical to those of ISORROPIA II in the metastable state, the results of the latter are not shown. The discussion of Section 3.3 has been extended to include the results of the ISORROPIA II evaluation, while the tables that contain the seasonal statistical analysis can be found in the updated supplement.

10. *Section 5, Page 25: It is not clear from the conclusions which version of ISORROPIA the authors propose to use for EMAC simulations. This section lacks an explanation as to why the stable mode was previously chosen for the model over the metastable mode, but now it is replaced with the metastable one. Is it only a matter of computational speed? A more detailed discussion would help.*

The aim of this study is not to propose one specific version of the ISORROPIA module over the other, but rather to demonstrate that ISORROPIA-lite is equally accurate in predicting inorganic aerosols with improved computational efficiency, and to provide insight into the conditions and regions where the results of the two available versions in EMAC might differ. In previous versions of the EMAC model, the stable mode was used as the default, mainly because it was thought to represent large desert regions more realistically due to their low annual RH values (Karydis et al., 2010; Karydis et al., 2016). However, the metastable assumption is often considered more accurate for regions such as the Northeastern US (Guo et al., 2016). The choice of the default setting is now mentioned at the end of Section 2.2, and a more detailed discussion of the advantages and disadvantages of each thermodynamic state and module is given in Section 4.

11. *Sect. 2.1, l.169 & Sect. 3.1 l. 216: The emissions of crustal ions such as Ca²⁺, Mg⁺, and K⁺, are calculated as a fraction of dust fluxes in the model. In what form these ions are emitted; totally or partially soluble/insoluble? Are these fractions directly inserted in ISORROPIA calculations? Do you also track in your model the different species upon the ISORROPIA call (e.g., CaSO₄)? In how many modes/sizes aerosol emissions are emitted in the model? Is ISORROPIA called for every aerosol mode/size or only for accumulation and coarse, as presented in the manuscript? If yes, how do you define here the fine aerosol acidity? Please discuss.*

Generally, crustal ions are emitted as partially soluble/insoluble in the accumulation and coarse modes and mostly in the insoluble fraction. For this study the mineral ions Ca²⁺, Mg⁺, and K⁺ were emitted as part of the dust flux in the insoluble fraction and in the accumulation and coarse size modes. All aerosol modes (4 soluble and 3 insoluble modes) are included in the ISORROPIA calculations as part of the system K⁺, Ca²⁺, Mg⁺, NH₄⁺, Na⁺, Cl⁻, NO₃⁻, SO₄²⁻ and H₂O. Insoluble particles are transferred to the soluble fraction after ISORROPIA calculations by coagulation with other soluble species, but mostly by condensation of water-soluble species (such as HNO₃) on their surface. EMAC tracks the concentration of all gaseous, liquid and solid species present in ISORROPIA, but the output is stored in the form of ions (e.g., SO₄²⁻, NO₃⁻, NH₄⁺, etc.) for each size mode. The above information has been added in Section 2 of the revised manuscript. Aerosol acidity is only estimated for the accumulation and coarse soluble size modes. This is now clarified in Section 4.3.

Technical Comments

12. *Page 2, l. 50: The transition from health-related issues to the climate impacts of aerosols is very steep.*

A connecting sentence has been added at this point in Section 1 to make the transition between health impacts and climate impacts easier for the reader.

13. *Figure 9: It would be easier for the reader to provide more details in the titles of the figures in the right column because negative pHs are acceptable values (not only for differences). A more detailed figure title can apply to all figures, especially when you show differences.*

Titles in all figures displaying differences between any two ISORROPIA versions have been changed to be as descriptive as possible, both in the revised manuscript and in the supplement.

References

- de Meij, A., Pozzer, A., Pringle, K. J., Tost, H., and Lelieveld, J.: EMAC model evaluation and analysis of atmospheric aerosol properties and distribution with a focus on the Mediterranean region, *Atmospheric Research*, 114-115, 38-69, <https://doi.org/10.1016/j.atmosres.2012.05.014>, 2012.
- Guo, H., Sullivan, A. P., Campuzano-Jost, P., Schroder, J. C., Lopez-Hilfiker, F. D., Dibb, J. E., Jimenez, J. L., Thornton, J. A., Brown, S. S., Nenes, A., and Weber, R. J.: Fine particle pH and the partitioning

- of nitric acid during winter in the northeastern United States. *Journal of Geophysical Research: Atmospheres*, 121, 10, 355-310, 376, <https://doi.org/10.1002/2016JD025311>, 2016.
- J. L. W. V. Jensen.: Sur les fonctions convexes et les inégalités entre les valeurs moyennes. *Acta Math.* 30, 175-193, <https://doi.org/10.1007/BF02418571>, 1906.
- Karydis, V. A., Tsimpidi, A. P., Pozzer, A., Astitha, M., and Lelieveld, J.: Effects of mineral dust on global atmospheric nitrate concentrations. *Atmospheric Chemistry and Physics*, 16(3), 1491-1509, <https://doi.org/10.5194/acp-16-1491-2016>, 2016.
- Karydis, V. A., Tsimpidi, A. P., Pozzer, A., and Lelieveld, J.: How alkaline compounds control atmospheric aerosol particle acidity. *Atmospheric Chemistry and Physics*, 21(19), 14983-15001, <https://doi.org/10.5194/acp-21-14983-2021>, 2021.
- Metzger, S., Abdelkader, M., Steil, B., and Klingmüller, K.: Aerosol water parameterization: long-term evaluation and importance for climate studies, *Atmospheric Chemistry and Physics*, 18, 16747-16774, <https://doi.org/10.5194/acp-18-16747-2018>, 2018.
- Pozzer, A., de Meij, A., Pringle, K. J., Tost, H., Doering, U. M., van Aardenne, J., and Lelieveld, J.: Distributions and regional budgets of aerosols and their precursors simulated with the EMAC chemistry-climate model, *Atmospheric Chemistry and Physics*, 12, <https://doi.org/10.5194/acp-12-961-2012>, 2012.
- Song, S., Gao, M., Xu, W., Shao, J., Shi, G., Wang, S. and co-authors: Fine-particle pH for Beijing winter haze as inferred from different thermodynamic equilibrium models. *Atmospheric Chemistry and Physics*, 18(10), 7423-7438, <https://doi.org/10.5194/acp-18-7423-2018>, 2018.

Authors' Response to Anonymous Referee's #2 Comments:

Summary:

This EMAC study investigates differences in aerosol modeling results using ISORROPIA II v1, ISORROPIA II v2.3, and ISORROPIA-lite. Notably, disparities in major aerosol components between ISORROPIA II v2.3 and ISORROPIA-lite are consistently less than 10%. Moreover, the application of ISORROPIA-lite results in a notable 5% acceleration in EMAC's computational performance. Despite ISORROPIA-lite's limitation to supersaturated aqueous (metastable) solutions, the authors endorse it as a dependable replacement for the previous thermodynamic module in EMAC. The paper's content is sufficiently detailed, and with the code now accessible through a Zenodo private repository, the manuscript could be considered for publication once all reviewer comments have been addressed. It's important to note that I concur with the specific comments made by referee 1 and won't reiterate them here.

We thank the reviewer for the positive review of our manuscript and the helpful comments. Below is a point-by-point response to his/her comments.

General Comments

- 1. Accuracy and Clarity: To ensure accuracy and clarity, it's essential to avoid misleading statements. While the results from ISORROPIA-lite are promising, its restriction to the metastable aerosol state renders it too limited for global atmospheric chemistry applications. This limitation could lead to errors in radiative forcing estimates, particularly in the free troposphere with low humidity. What is really needed are codes that can capture the hysteresis effect of aerosols in order to improve aerosol radiative forcing effects. Therefore, the statement that "ISORROPIA-lite can be a reliable and computationally effective replacement of the previous thermodynamic module in EMAC" should be approached with caution, pending a thorough evaluation of its suitability for global applications.*

ISORROPIA-lite should not be considered as a replacement for the ISORROPIA-II stable mode, but rather as an alternative version of the model that can be selected by the user depending on the application and the desired efficiency and/or state assumption. The aim of this study is to demonstrate that ISORROPIA-lite is equally accurate in predicting inorganic aerosol composition with improved computational efficiency and to provide insight into the conditions and regions where the results of the two versions available in EMAC might differ. However, it should be emphasized that the stable assumption should not always be considered as more accurate. During simulations, atmospheric particles are transported from one simulated cell to another by simultaneously undergoing several atmospheric processes that change their chemical composition. In many cases, they end up in computational cells with completely different RH without "carrying" their historical RH profile with them. Therefore, the choice between a stable state (e.g., following the deliquescence branch of crystallization) and a metastable state (following the efflorescence branch) should not be considered obvious. While a stable state could be considered more accurate under very low humidity conditions (e.g., over remote deserts), in regions, such as those with intermediate RH and low nitrate concentration (e.g., Northeastern US), particles are mostly in metastable state. However, the two state assumptions produce very similar results in most cases, as shown in our study. Overall, following the reviewer's comment, we have enriched our discussion in Sections 2, 4, and 5 of the revised manuscript by avoiding statements that could lead to confusion about the climatic impacts of the two model versions.

2. **Omission of References:** *The omission of references to relevant thermodynamic codes commonly used within EMAC is a notable gap in the introduction, potentially impacting the manuscript's scientific credibility. It's crucial to acknowledge and cite widely accepted models, following established conventions in scientific publishing.*

We thank the reviewer for pointing this out. Indeed, EQSAM is the other available option besides ISORROPIA in the EMAC model for aerosol thermodynamic calculations and is now described in the introduction. We also clarify that EQSAM is still an available option in EMAC.

3. **Consistency:** *Ensure consistency in the spelling of "ISORROPIA-lite" and other acronyms throughout the text to maintain clarity and professionalism.*

All the acronyms used in the manuscript have been thoroughly revised.

Specific Comments:

1. **Discussion of Activity Coefficient:** *If tabulated activity coefficients are mentioned, it's crucial to provide a clear and comprehensive explanation or reference regarding their origin and relevance. This will ensure that readers fully understand their context.*

The use of tabulated activity coefficients (by ISORROPIA II and ISORROPIA-lite) is now explained in Section 2.2. The methodology for their calculation is briefly presented, with all relevant references cited (Kusik and HP (1978); Bromley (1973); Meissner and Peppas (1973)). Further information can be found in Fountoukis and Nenes (2007).

2. **Temporal Analysis:** *In Table 2, where annual means of surface concentrations are discussed, it's worth noting that a 5% difference on an annual scale can translate to significantly higher variations when considering shorter timeframes, such as hourly averages, commonly used in air quality applications. To enhance the analysis, consider extending the statistical examination to at least daily values at a regional scale, focusing on selected networks. Relying solely on mean annual concentrations limits the scope of the analysis and its conclusion.*

Tables 1,2 and 7, in Sections 3.1, 3.2, and 4.1, respectively, which presented the statistical comparison between the model estimates of the different ISORROPIA versions, have been updated to include the daily averages. The box plots in Figures 7, S1 and S2, show the regional differences of the estimated daily average coarse and fine NO_3^- concentrations by the different ISORROPIA versions for five specific regions. The regional analysis focuses on the differences in NO_3^- concentrations since this is the aerosol component with the highest discrepancy between the different ISORROPIA versions.

3. **Computational Speed-Up Analysis:** *The metric presented in Table 6 regarding computational speed-up should ideally encompass information about load imbalances within the system or undergo a more rigorous statistical analysis. To strengthen the analysis, consider running multiple iterations for each version to draw more robust and conclusive findings. As currently presented, the analysis is relatively weak, and its conclusions are somewhat limited.*

The statistics presented in Table 6 have been updated to include not only the results of a single simulation for each version, but a total of 18 simulations (6 for each version). The revised table 6 shows the average values of the statistical metrics used, as well as their standard deviation.

4. ***Section 4 Focus on Surface Concentrations:*** *Section 4 predominantly concentrates on surface concentrations, which may not offer a comprehensive evaluation of the metastable effect as intended by the authors. Consider revising the analysis in Section 4 to include an assessment of the vertical integral (burden) and, at the very least, a comparison of zonal means. The current presentation may be misleading without these additional elements.*

An assessment of the tropospheric burden of total NO_3^- aerosol between the two ISORROPIA versions can be found in Section 4.1. The analysis has now been extended to include the zonal mean annual concentrations of all aerosol components and their deviation between ISORROPIA II and ISORROPIA-lite (Figures S3 and S5 in the revised supplement). We found that the deviations between the results of the two ISORROPIA versions are becoming smaller as the air masses move higher in the atmosphere, until they are practically identical at altitudes above 700hPa. The discussion in Section 4.1 has been extended accordingly.

5. ***References and Errata:*** *Ensure that references are not duplicated and address any missing errata. This will enhance the overall quality of the document and its accuracy.*

The reference list has been thoroughly revised.

REFERENCES

- Bromley, L. A.: Thermodynamic properties of strong electrolytes in aqueous solutions. *AIChE journal*, 19(2), 313-320, <https://doi.org/10.1002/aic.690190216>, 1973.
- Fountoukis, C. and Nenes, A.: ISORROPIA II: a computationally efficient thermodynamic equilibrium model for K^+ – Ca^{2+} – Mg^{2+} – NH_4^+ – Na^+ – SO_4^{2-} – NO_3^- – Cl^- – H_2O aerosols. *Atmospheric Chemistry and Physics*, 7(17), 4639-4659, <https://doi.org/10.5194/acp-7-4639-2007>, 2007
- Kusik, C. and HP, M. 1978. Electrolyte Activity Coefficients in Inorganic Processing. *AIChE Symp. Series*, 173, 14-20, 1978.
- Meissner, H. P. and Peppas, N. A.: Activity coefficients – aqueous solutions of polybasic acids and their salts, *AIChE Journal*, 19(4), 806–809, <https://doi.org/10.1002/aic.690190419>, 1973.

Implementation of the ISORROPIA-lite Aerosol Thermodynamics Model into the EMAC Chemistry Climate Model (based on MESSy v2.55): Implications for Aerosol Composition and Acidity

Alexandros Milousis¹, Alexandra P. Tsimpidi¹, Holger Tost², Spyros N. Pandis^{3,4}, Athanasios Nenes^{3,5}, Astrid ~~Kiedler~~Kiendler-Scharr¹⁺, and Vlassis A. Karydis¹

¹Forschungszentrum Jülich GmbH, Institute for Energy and Climate Research, IEK-8 Troposphere, Jülich, Germany

²Johannes Gutenberg University Mainz, Institute of Atmospheric Physics, Mainz, Germany

³FORTH ICE HT, Institute of Chemical Engineering Sciences, Patras 26504, Greece

⁴University of Patras, Department of Chemical Engineering, Patras 26500, Greece

⁵Ecole Polytechnique Fed Lausanne, School of Architecture Civil & Environmental Engineering Lab, Atmospheric Processes & Their Impacts, CH-1015 Lausanne, Switzerland

⁺deceased

Correspondence to: Vlassis Karydis (v.karydis@fz-juelich.de)

Abstract. This study explores the differences in performance and results by various versions of the ISORROPIA thermodynamic module implemented within the global atmospheric chemistry model EMAC. Three different versions of the module were used, ISORROPIA II v1, ISORROPIA II v2.3, and ISORROPIA-lite. First, ISORROPIA II v2.3 replaced ISORROPIA II v1 in EMAC to improve pH predictions close to neutral conditions. The newly developed ISORROPIA-lite has been added to EMAC alongside ISORROPIA II v2.3. ISORROPIA-lite is more computationally efficient and assumes that atmospheric aerosols exist always as supersaturated aqueous (metastable) solutions while ISORROPIA II includes the option to allow the formation of solid salts at low RH conditions (stable state). The predictions of EMAC by employing all three aerosol thermodynamic models were compared to each other and evaluated against surface measurements from three regional observational networks (IMPROVE, EMEP, EANET) in the polluted Northern Hemisphere. The differences between ISORROPIA II v2.3 and ISORROPIA-lite were minimal in all comparisons with the normalized mean absolute difference for the concentrations of all major aerosol components being less than 11% even when different phase state assumptions were used. The most notable differences were lower aerosol concentrations predicted by ISORROPIA-lite in regions with relative humidity in the range of 20% to 60% compared to the predictions of ISORROPIA II v2.3 in stable mode. The comparison against observations yielded satisfactory agreement especially over the US and Europe, but higher deviations over East Asia, where the overprediction of EMAC for nitrate was as high as $4 \mu\text{g m}^{-3}$ (~ 20%). The mean annual aerosol pH predicted by ISORROPIA-lite was on average less than a unit lower than ISORROPIA II v2.3 in stable mode, mainly for coarse mode aerosols over Middle East. The use of ISORROPIA-lite accelerated EMAC by nearly 5% compared to the use of ISORROPIA II v2.3 even if the aerosol thermodynamic calculations consume a relatively small fraction of the EMAC computational time. ISORROPIA-lite can therefore be a reliable and computationally effective replacement of efficient alternative to the previous thermodynamic module in EMAC.

Keywords: atmospheric aerosols, aerosol thermodynamics, nitrate, acidity, aerosol phase state.

1. Introduction

Aerosols in the atmosphere have a significant impact on climate and air pollution. They contribute to the deterioration of air quality, especially in heavily industrialised regions, leading to increased mortality rates and decreased life expectancy (Heroux-Héroux et al., 2015). Particulate matter with diameter less than 2.5 μm ($\text{PM}_{2.5}$) is the largest contributor to stroke, cancer, heart conditions and chronic obstructive pulmonary diseases (Brook et al., 2010; Pope et al., 2011) with ambient pollution causing approximately 4.2 million premature deaths in 2019 alone (WHO, 2022). Tarin-Carrasco et al. (2021) predicted that mortality rates in Europe due to air pollution could increase in the next thirty years in the more extreme emission scenarios (e.g., RCP8.5). Aerosols in addition to the direct threat aerosols pose to humans and ecosystems through their effects on air quality, they can also affect other climate-related processes. For example, they can act as cloud condensation nuclei and by altering modify cloud lifetime and optical properties (Andreae et al., 2005; Klingmüller et al., 2020). They also affect the energy balance of our planet by reflecting additional solar radiation back to space and thus cooling the atmosphere or by absorbing solar radiation warming the atmosphere (Klingmüller et al., 2019; Miinalainen et al., 2021). Some major inorganic aerosol components also affect various ecosystems. For example, nitrates and sulfates can harm flora by lessening its lifetime and variety (Honour et al., 2009; Manisalidis et al., 2020), and can affect wildlife by causing water eutrophication (Doney et al., 2007). A critical property of atmospheric particles that regulates their impacts on clouds and ecosystems is their acidity (Karydis et al., 2021). Depending on its levels, acidity can affect air quality and human health (Lelieveld et al., 2015) but also the aerosols' hygroscopic characteristics (Karydis et al., 2016). The aerosol pH also drives the partitioning of semi-volatile inorganic components between the gas and aerosol phases (Nenes et al., 2020). Finally, aerosol acidity plays a role in the activation of halogens in aerosols (Saiz-Lopez and von Glasow, 2012), their toxicity (Fang et al., 2017) and also in secondary organic aerosol formation (Marais et al., 2016).

Sulfate is the most important component of $\text{PM}_{2.5}$ inorganic aerosol, since it contributes the most in terms of global mass burden (Szopa et al., 2021) and aerosol optical depth (AOD) (Myhre et al., 2013). Nitrate contribution to the $\text{PM}_{2.5}$ aerosol composition is also important in several areas (e.g., Europe, North America, East Asia) and seasons (He et al., 2001; Silva et al., 2007; Weagle et al., 2018; Tang et al., 2021). The quantification of nitrate partitioning between the gas and particulate phases is challenging partly because it is affected by meteorology (temperature, relative humidity) and all ionic aerosol components, but also due to the lack of observations to constrain the composition of the gas-phase components and the size-distribution of the particulate phase. Nitrate in the form of ammonium nitrate is mainly found in the fine mode (e.g., $\text{PM}_{2.5}$) (Putaud et al., 2010). This is especially the case over polluted regions where there is enough ammonia remaining after the neutralization of sulfate (Karydis et al., 2011; Karydis et al., 2016). In coastal and desert areas, nitrate is formed mainly by reactions of HNO_3 with sea salt and dust particles (Savoie and Prospero, 1982; Wolff, 1984; Karydis et al., 2016) and therefore is found mainly in the coarse particles. The importance of nitrate in the troposphere is expected to increase in the following decades because SO_2 emissions are anticipated to drop while NH_3 emissions to increase (Fu et al., 2017; Chen et al., 2019; Xu et al., 2020). With decreased SO_2 concentrations,

less ammonia is required to neutralize the sulfates and therefore more is available for ammonium nitrate formation (Tsimpidi et al., 2007). (Tsimpidi et al., 2007).

There have been several ~~thermodynamical~~thermodynamic models developed in the last decades to calculate the inorganic aerosol concentrations and composition in the atmosphere. Two of the first were EQUIL and KEQUIL developed by Bassett and Seinfeld (1983). Then the MARS model was developed by Saxena et al. (1986) with the aim of reducing the computational time required in order to be incorporated into larger scale chemical transport models. MARS was the first model to divide the composition domain into smaller sub-domains aiming to reduce the number of equations needed to be solved. Then the SEQUILIB model by Pilinis and Seinfeld (1987) was the first to incorporate sodium and chloride and the corresponding salts in the simulated aerosol system. Further developments included EQUISOLV by Jacobson et al. (1996) as well as SCAPE by Kim et al. (1993), which simulated temperature dependent deliquescence following Wexler and Seinfeld (1991) and predicted the presence of liquid phase aerosols even at low relative humidity (RH). E-AIM is another benchmark thermodynamic model which instead of solving algebraic equations for equilibrium, uses the minimization of the Gibbs Free Energy approach (Wexler and Clegg, 2002). Later versions of E-AIM also include selected organic aerosol components (Clegg et al., 2003). Furthermore, AIOMFAC is a model that utilizes organic-inorganic interactions in aqueous solutions in order to calculate activity coefficients up to high ionic strengths (Zuend et al., 2008) and is based on the LIFAC model by Yan et al. (1999). Further developments in AIOMFAC include a wider variety of organic compounds (Zuend et al., 2011). The EQSAM thermodynamic model was developed by Metzger et al. (2002) with the basic concept that aerosol activities in equilibrium are controlled by RH, and solute activity is a function of RH. The model uses a domain structure based on sulphate availability to increase computational efficiency by solving fewer thermodynamic equations, similar to Nenes et al. (1998). EQSAM and ISORROPIA are the two available options for aerosol thermodynamics in the EMAC model.

Nenes et al. (1998) developed the ISORROPIA model in an effort to increase computational efficiency while maintaining the accuracy of the calculations. The system simulated by ISORROPIA included NH_4^+ , Na^+ , Cl^- , NO_3^- , SO_4^{2-} and H_2O . ISORROPIA also contains the temperature dependent equations for deliquescence by Wexler and Seinfeld (1991) and is computationally efficient so that it can be incorporated in 3D atmospheric models. In ISORROPIA, the aerosol state is predicted as a weighted mean value of the dry and wet states. The weighting factors depend on ambient RH, the mutual deliquescence relative humidity (MDRH) and the deliquescence relative humidity (DRH) of the most hygroscopic salt in the mixture. An improved version of ISORROPIA including the mineral ions K^+ , Ca^{2+} , and Mg^{2+} , called ISORROPIA II, was developed by Fountoukis and Nenes (2007). The addition of the above crustal ions resulted in the inclusion of 10 more salts and 3 more ions in the solid and aqueous phases respectively. The model gained in computational efficiency by performing different calculations for different atmospheric chemical composition regimes ~~and by using pre-calculated look-up tables for the activity coefficients,~~ which are determined by the abundance of each aerosol precursor as well as the ambient temperature and relative humidity. Depending on the values of the so-called 'sulfate ratio', the 'crustal species and sodium ratio' and the 'crustal species' ratio, five aerosol composition regimes are determined in order to calculate the necessary equilibrium equations for the species present in each regime. Furthermore, the use of pre-calculated look-up tables for the activity

[coefficients \(see Section 2.2\), including their temperature dependence, is another factor for the gain in computational efficiency.](#) Like E-AIM, ISORROPIA II can solve the thermodynamic equilibrium problem under stable or metastable conditions. In the second case aerosols are assumed to exist only as supersaturated aqueous solutions even at low RH, while in the first the aerosols are able to form solid salts. A very slightly updated version, called ISORROPIA II v2.3 was introduced to improve aerosol pH predictions close to neutral conditions (Song et al., 2018). [More specifically, in some subcases of the ISORROPIA II regime, NH₃ evaporation was not taken into account in the aerosol pH calculations, leading to unrealistic estimates close to neutrality \(pH~7\). This error had a minimal effect on the predicted gas phase NH₃ levels and consequently on the inorganic aerosol concentrations. Moreover, it only affected a few subcases and only when the stable mode was used. More details on these differences can be found in Song et al. \(2018\).](#) The newest development of ISORROPIA II, called ISORROPIA-lite, was designed to be even more computationally efficient than its predecessor and to also include the effects that organic aerosol components have on particle water and the semi volatile inorganic aerosol species partitioning (Kakavas et al., 2022).

This study aims to evaluate the newly developed ISORROPIA-lite thermodynamic module within the EMAC global climate and chemistry model and to explore any discrepancies on a global scale, by utilizing different aerosol phase states. For this reason, our analysis explores the differences in the results between ISORROPIA-lite and ISORROPIA II over diverse conditions and environments. In Section 2 the model configuration and the treatment of inorganic aerosols thermodynamics is presented. In Sections 3 and 4 the results and comparisons between the simulations are analyzed and in Section 5 the major conclusions are presented.

2. Model Configuration

2.1 EMAC model setup

The EMAC (ECHAM5/MESSy) model is a global atmospheric chemistry and climate model (Jockel et al., 2006). It includes a series of submodels and links them via the Modular Earth Submodel System ([Jöckel, Jöckel et al., 2005](#)) to the base model (core) that is the 5th generation European Center Hamburg general circulation model (Roeckner et al., 2006). Gas-phase chemistry is simulated by MECCA (Sander et al., 2019) with a simplified scheme similar to the one used in CCMI (Chemistry-Climate Model Initiative) like in Jockel et al. (2016). Aerosol microphysics along with gas/aerosol partitioning are treated by GMXe in which the aerosols are differentiated between soluble and insoluble modes with a total of seven lognormal modes (Pringle et al., 2010). The soluble mode contains the nucleation, Aitken, accumulation, and coarse size ranges while the insoluble mode lacks only the nucleation size range. Transfer of material between the insoluble and soluble modes is calculated in two processes. After coagulation, when a hydrophobic and a hydrophilic particle coagulate, the resulting mass is assumed to reside in the hydrophilic mode and also when soluble material condenses onto a hydrophobic particle (after gas/aerosol partitioning)

it is again transferred to the hydrophilic mode (Pringle et al., 2010). Wet deposition of gases and aerosols is described by SCAV (Tost et al., 2006; 2007), dry deposition via DRYDEP (Kerkweg et al., 2006) and gravitational sedimentation of aerosols by SEDI (Kerkweg et al., 2006). Cloud properties and microphysics are calculated by the CLOUD submodel (Roeckner et al., 2006) utilizing the detailed two-moment liquid and ice-cloud microphysical scheme of Lohmann and Ferrachat (2010) and considering a physically based treatment of the processes of liquid (Karydis et al., 2017) and ice crystals (Bacer et al., 2018) activation. The organic aerosol composition and evolution in the atmosphere is calculated by the ORACLE submodel (~~Tsimpidi et al., 2014, 2018~~)(Tsimpidi et al., 2014; 2018).

The model simulations in this work were nudged towards actual meteorology using ERA05 data (Hersbach et al., 2020). For the purposes of this study the spectral resolution applied within EMAC was the T63L31 which corresponds to a grid resolution of $1.875^\circ \times 1.875^\circ$, covering ~~vertically~~vertical altitudes up to 25 km with a total of 31 layers. The simulations were all done for the period 2009-2010, with 2009 representing the model spin-up period.

Anthropogenic emissions of aerosols and aerosol precursors were based on the EDGARv4.3.2 inventory (Crippa et al., 2018). Open biomass burning emissions were derived by the GFEDv3.1 database (van der Werf et al., 2010), and natural emissions of NH_3 (volatilization from soils and oceans) were based on the GEIA database (Bouwman et al., 1997). SO_2 emissions by volcanic eruptions are based on the AEROCOM dataset (Dentener et al., 2006), as are emissions of sea spray aerosols using the chemical composition proposed by Seinfeld and Pandis (2016). Biogenic emissions of NO from soils are calculated online according to the algorithm of Yienger and Levy (1995) while NO_x produced by lightning is also calculated online based on the parameterization of Grewe et al. (2001). Oceanic emissions of DMS are calculated online by the AIRSEA submodel (Pozzer et al., 2006). Finally, the dust emission fluxes are calculated online according to Astitha et al. (2012), by taking into account the meteorological information for each grid cell (i.e., temperature and relative humidity) as well as the different thresholds of friction velocities above which suspension of dust particles takes place. The emissions of crustal ions (Ca^{2+} , Mg^+ , K^+ and Na^+) are estimated as a fraction of the total dust flux based on the soil chemical composition of each individual grid cell (Karydis et al., 2016; Klingmüller et al., 2018). These ions are emitted in the insoluble accumulation and coarse size modes and are subsequently transferred to the soluble aerosols by the processes described above.

2.2 Inorganic aerosol thermodynamics treatment

In this study, the ISORROPIA-lite aerosol thermodynamic model has been implemented into the EMAC as part of the GMXe submodel, not as a replacement but as an alternative to the previous version, in order to efficiently calculate the equilibrium partitioning of the inorganic species between gas and aerosol phases. Furthermore, ISORROPIA II v2.3 is used to replace ISORROPIA II v1 in the model.

Kinetic limitations in the partitioning need to be taken into consideration because only fine aerosols are able to achieve equilibrium within the time frame of one model time step, which in this study equals to 10 minutes. Therefore, the partitioning calculation is done in two stages according to Pringle et al. (2010). First the amount of the gas-phase species that is able to

kinetically condense onto the aerosol phase within the model time step is calculated by assuming diffusion limited condensation (Vignati et al., 2004). Then in the second stage, the partitioning between this gas phase material and the aerosol phase is performed. The partitioning calculation is performed for all seven size modes, i.e. in each model timestep ISORROPIA is called separately for each of them.

According to Kakavas et al. (2022), ISORROPIA-lite features two main modifications in its code, with regard to ISORROPIA II v2.3 (Song et al., 2018) and ISORROPIA II v1 (Fountoukis and Nenes, 2007). First, the routines related to the stable case have been removed, since only the metastable case is considered- and all salts formed are deliquesced. However, CaSO₄ is the only solid salt allowed to form, as it is considered insoluble for most atmospherically-relevant RH values and precipitates spontaneously. Furthermore, for the calculation of ~~the~~ binary activity coefficients, ~~ISORROPIA~~ ISORROPIA-lite uses the tabulated binary activity coefficient data for each salt ~~by~~from Kusik-Meissner (Kusik and Meissner, 1978) instead of ~~computing~~calculating them online, and includes their temperature dependence according to Meissner and Peppas (1973). This is done by combining the Kusik and ~~HP~~Meissner (1978) model for specific ionic pairs with the Bromley (1973) activity ~~coefficients~~coefficient mixing rule for multicomponent mixtures. More information on this procedure, can be found in Fountoukis and Nenes (2007). This second modification is the major contributor to the computational speed-up provided by ISORROPIA-lite, which in an offline estimation was reported to be around 35% (Kakavas et al., 2022). Furthermore, this feature could explain differences in inorganic aerosol estimates with the previous version of ISORROPIA using the same aerosol state assumption (metastable case). Another important modification is that the effect of organic aerosol water on the inorganic semi volatile aerosol components is included. This consideration slightly increases the aerosol pH but more significantly drives the phase partitioning towards the aerosol phase in order to satisfy equilibrium conditions (Kakavas et al., 2022). However, this feature of ISORROPIA-lite was not used in the present study, as the water uptake by organics is treated by other parts of the GMXe aerosol microphysics submodel in the EMAC global model. The effects of the secondary organic aerosol on aerosol water and nitrate partitioning are discussed by Kakavas et al. (2023).

In the updated version of the GMXe submodel, the users have the option to select between ISORROPIA-lite- and ISORROPIA II v2.3 to perform EMAC simulations depending on the application and the desired phase state assumption. While ISORROPIA-lite utilizes the metastable approach exclusively, ISORROPIA II v2.3 utilizes both and has the stable approach as default.

3. Evaluation of New Aerosol Thermodynamic Modules within EMAC

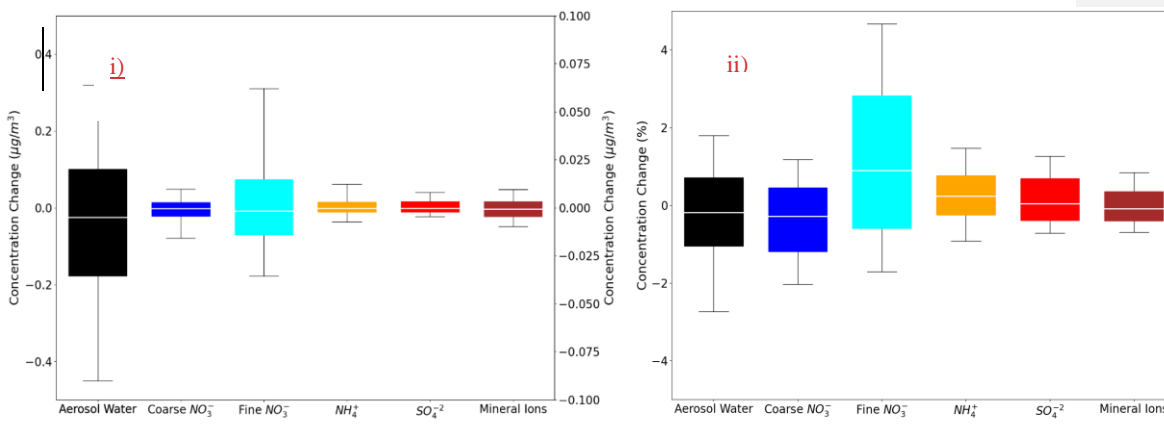
For reasons of clarity, from this point forward both in the main text as well as in any figure captions, whenever different aerosol sizes are mentioned, total suspended particles (TSP) refer to the sum of the 4 lognormal size modes of the aerosol microphysics submodel (i.e. nucleation, Aitken, accumulation and coarse mode), fine aerosols refer to the sum of the 3 smaller size modes (nucleation, Aitken and accumulation mode) and coarse aerosols refer to the largest size mode of the model exclusively.

3.1 Comparison of ISORROPIA II v1 against ISORROPIA II v2.3 in stable mode

The first comparison aims to examine how ISORROPIA II v2.3 fares against ISORROPIA II v1 when considering solely the stable assumption, after the latter's replacement in the newer version of the EMAC model.

The differences in global daily mean surface concentrations of NH_4^+ , SO_4^{2-} , mineral ions (sum of Ca^{2+} , K^+ , Mg^{+2}), aerosol water in TSP, as well as fine and coarse aerosol NO_3^- as predicted by the two versions can be seen in Figure 1. The 25th and 75th percentiles of concentration differences between the two versions for the aerosol water are below $0.2 \mu\text{g m}^{-3}$ and for the remaining species they are an order of magnitude less, which translates to differences mostly below 2.51 % for all species. Therefore, the predictions of inorganic aerosol composition of the two versions agree exceptionally well.

In order to investigate potential differences arising in specific areas, regions affected by high nitrate concentrations were selected, i.e., Europe, the Tibetan Plateau, Eastern Asia, North America and the Middle East. The differences in daily mean coarse and fine NO_3^- over these regions are shown in Figure S1. The comparison showed that the differences regarding the 25th and 75th percentiles are less than $0.05 \mu\text{g m}^{-3}$ (or less than 2.5 %) between the results of the two ISORROPIA II versions for both size modes. A statistical analysis of the results reveals that all differences between the aforementioned species are on average below 23% (Table 1). Therefore, the replacement of ISORROPIA II v1 by v2.3 in the EMAC model yields only trivial differences in the predicted aerosol ionic composition and water. The following sections focus on the comparison between the results of ISORROPIA-lite against ISORROPIA II v2.3 (called ISORROPIA II hereafter for simplicity), both in stable and metastable states.



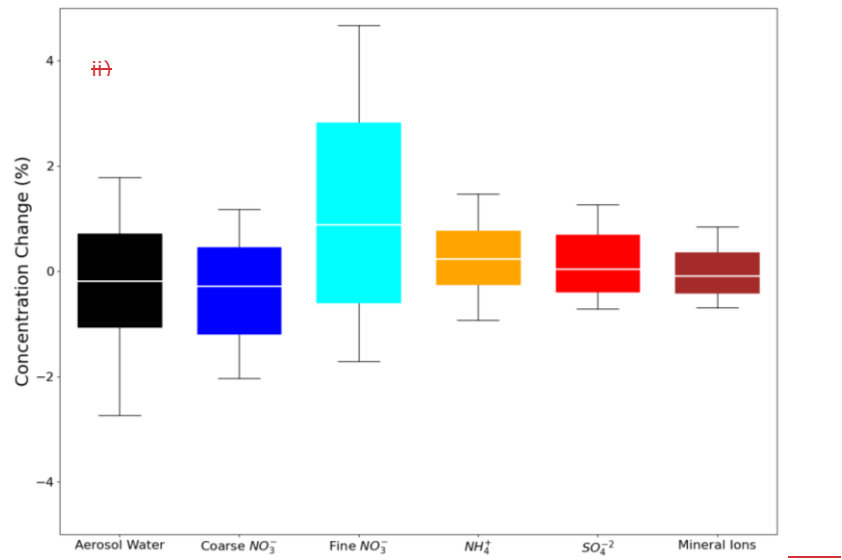
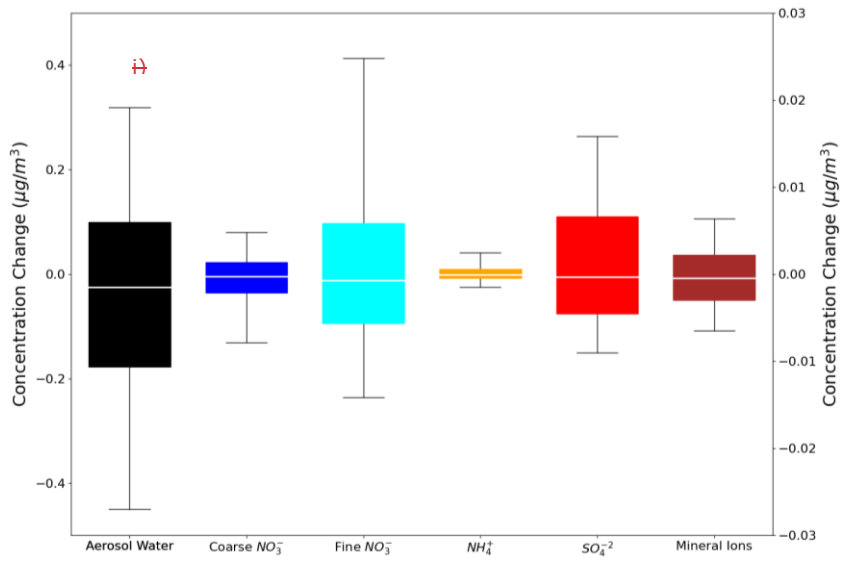


Figure 1: Bar chart plots depicting the 25th, 50th and 75th percentiles (box) of the i) difference and ii) fractional difference in global daily mean surface concentrations of aerosol water (left y-axis), mineral ions, NH₄⁺ and SO₄²⁻ in TSP as well as coarse and fine aerosol NO₃⁻ (right y-axis), as predicted by EMAC using ISORROPIA II v1 and ISORROPIA II v2.3. The 10th and 90th percentiles (whiskers) for each aerosol component are also shown. Both models assume that the aerosol is at its stable state at low RH and a positive change corresponds to higher concentrations by ISORROPIA II v1.

Table 1: Statistical analysis of EMAC-simulated mean ~~annual~~daily surface concentrations by employing ISORROPIA II v1 versus ISORROPIA II v2.3, both in **stable mode**. Deviations are given as ISORROPIA II v1 – ISORROPIA II v2.3.

	Mean Difference ($\mu\text{g}/\text{m}^3$)	Normalized Mean Absolute Difference (%)
Coarse NO ₃ ⁻	-8x10⁻⁴	1.8
Fine NO ₃ ⁻	-0.004011	2.6
HNO ₃ (g)	-0.005	0.7
NH ₄ ⁺	-9x10 ⁻⁴	2.40
SO ₄ ²⁻	-3x10³ 3.1x10 ⁻⁴	1.2
Na ⁺	-0.003	1.6
Ca ²⁺	0.002	0.7
K ⁺	3x10¹ 1.6x10 ⁻⁴	0.4
Mg ⁺	2x10⁻¹ 0.009	0.54
Cl ⁻	0.007	0.54
H ₂ O	1.7x10 ⁻⁴	0.5
H ⁺	3x10¹ 1.1x10 ⁻⁴	0.5
	0.028	2.3
	1.5x10 ⁻⁴	1.6
	0.040	0.8
	4x10⁰ 0.046	1.3
	-2.9x10 ⁻⁵	1.5

Formatted: Not Highlight

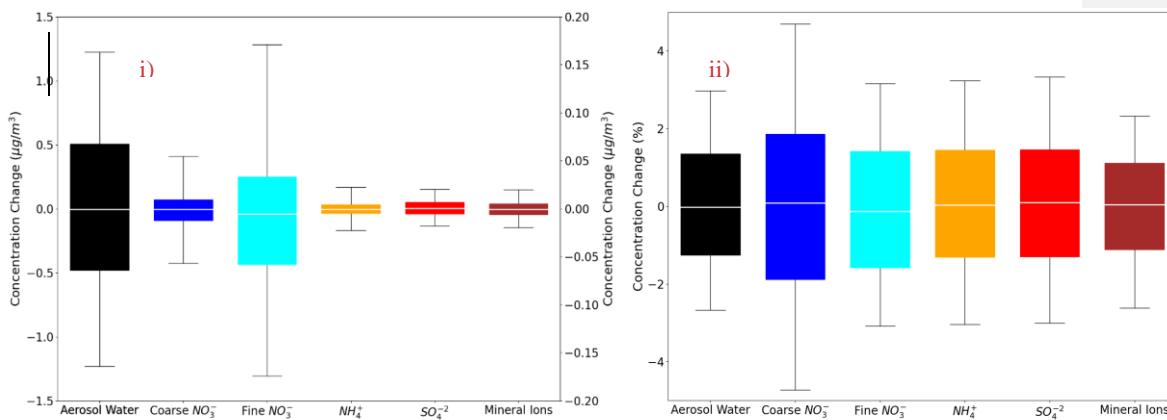
Formatted: Highlight

3.2 Comparison of ISORROPIA-lite against ISORROPIA II in metastable mode

The model results using ISORROPIA-lite are compared first against those using ISORROPIA II in metastable mode in order to determine whether the ISORROPIA-lite version can produce similar results with the more detailed module in EMAC, under same conditions. Figure 2 depicts the differences of the global daily mean surface concentrations of the same species that were examined before. The comparison yields differences for the 25th and 75th percentiles smaller than are less than $0.5 \mu\text{g m}^{-3}$ for the aerosol water and smaller, mostly less than $0.0405 \mu\text{g m}^{-3}$ for the remaining inorganic aerosol components, which translates into differences of less than 2% for all species most of the time.

Figure S2 shows the comparison between predicted global daily mean coarse and fine aerosol nitrate concentrations, focusing on the regions with the higher simulated mean annual concentrations. Across all regions, the concentration differences for both size modes are typically lower than $0.1 \mu\text{g m}^{-3}$ (or less than 3 %) and are mostly found over the Himalayan and East Asian regions.

In Table 2, the statistics of the results for the global surface concentrations for all examined aerosol components, reveal differences that are on average less than 57%. Therefore, ISORROPIA-lite does provide quite similar predictions with ISORROPIA II in the EMAC model, for simulations using the metastable state assumption.



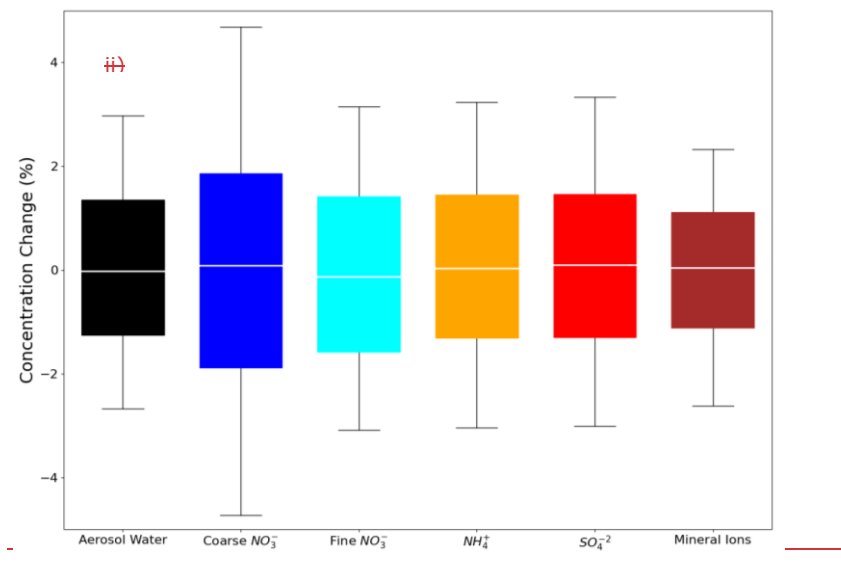
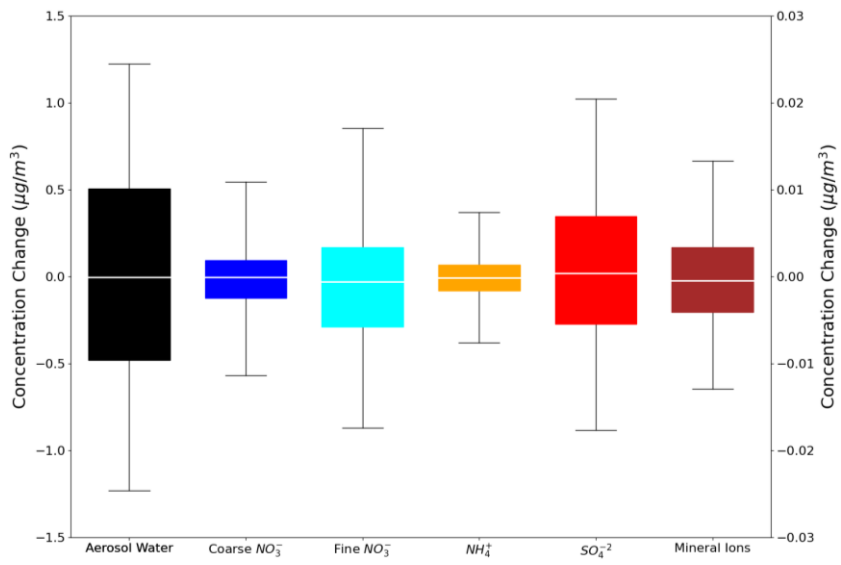


Figure 2-3 : Bar chart plots depicting the 25th, 50th and 75th percentiles (box) of the i) difference and ii) fractional difference in global daily mean surface concentrations of aerosol water (left y-axis), mineral ions, NH₄⁺ and SO₄²⁻ in TSP as well as coarse and fine aerosol NO₃⁻ (right y-axis) , as predicted by EMAC using ISORROPIA-lite and ISORROPIA II. The 10th and 90th percentiles (whiskers) for each aerosol component are also shown. Both models assume that the aerosol is at its metastable state at low RH and a positive change corresponds to higher concentrations by ISORROPIA-lite.

Formatted: Font: Bold, Underline

Table 2: Statistical analysis of EMAC-simulated mean ~~annual~~daily surface concentrations by employing ISORROPIA-lite versus ISORROPIA II, both in **metastable mode**.

Bias is given as ISORROPIA-lite – ISORROPIA II.

	Mean Difference ($\mu\text{g}/\text{m}^3$)	Normalized Mean Absolute Difference (%)
Coarse NO_3^-	-7×10^{-4}	<u>3.5</u>
Fine NO_3^-	-6.2×10^{-4}	<u>3.9</u>
HNO_3	-3.1×10^{-4}	<u>2.0</u>
NH_4^+	-2.7×10^{-4}	<u>3.8</u>
SO_4^{2-}	-1.4×10^{-5}	<u>4.0</u>
Na^+	2.5×10^{-3}	<u>6.7</u>
Ca^{2+}	<u>0.011</u>	1.9
K^+	2.9×10^{-4}	<u>2.4</u>
Mg^+	<u>1.8×10^{-4}</u>	<u>3.5</u>
Cl^-	-3×10^{-5}	<u>7.0</u>
H_2O	9×10^{-4}	1
H^+	0.004	2.8
	4×10^{-4}	2.7
	3×10^{-4}	2.3
	8×10^{-4}	2.3
	7×10^{-4}	4.2
	0.008017	2.3
	0.028035	2.8
	-1×10^{-5}	3.7
	8.3×10^{-4}	4.3
		1.5
		4.6

Formatted: Not Superscript/ Subscript

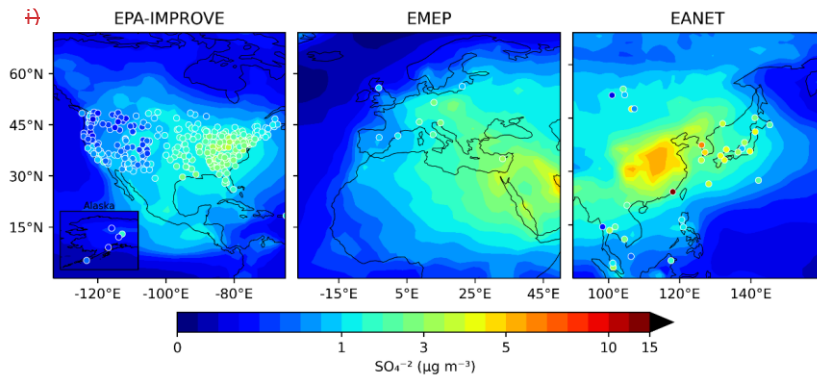
3.3 Evaluation of inorganic aerosol predictions

The EMAC predictions using both ISORROPIA-lite and ISORROPIA II in stable mode for $\text{PM}_{2.5}$ ammonium, sulfate and nitrate were compared against measurements from three observational networks. The networks cover some of the most polluted areas in the Northern Hemisphere. The EPA CASTNET network (U.S. Environmental Protection Agency Clean Air Status and Trends Network) and the IMPROVE network (Interagency Monitoring of Protected Visual Environments) with 152 stations for nitrate and sulfate and 143 stations for ammonium cover the USA, with IMPROVE concerning mostly rural and/or remote areas. The EMEP network (EMEP Programme Air Pollutant Monitoring Data) includes 9 stations for nitrate and sulfate and 7 for ammonium

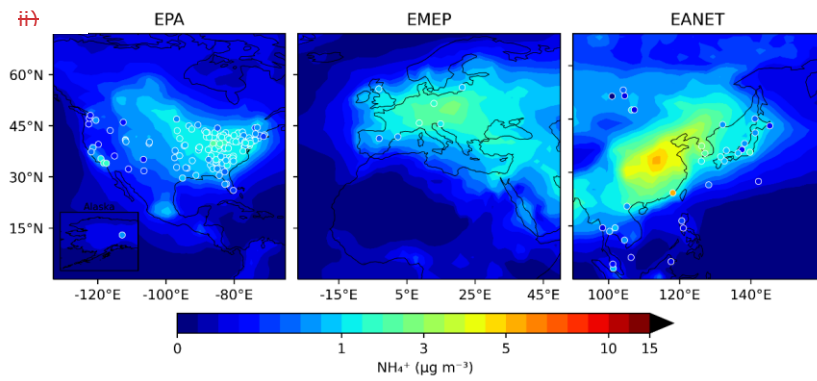
covering the European region. Finally, the EANET network (The Acid Deposition Monitoring Network in East Asia) with 33 stations measuring all three major aerosol components covers parts of East Asia. The number of stations refers to the year 2010 which is simulated in this work.

Figure 3 depicts the differences between the model-predicted and the observed mean annual concentration values for SO_4^{2-} , NH_4^+ and NO_3^- aerosols, while Tables 3, 4 and 5 contain the overall statistics for the same comparisons. Here, the mean bias (MB), mean absolute gross error (MAGE), normalized mean bias (NMB), normalized mean error (NME), and the root-mean-square error (RMSE) are calculated to assess the model performance. Starting with SO_4^{2-} , the model tends to underpredict the observations but with mean bias (MB) less than $-0.5 \mu\text{g m}^{-3}$ for Europe and less than $-1 \mu\text{g m}^{-3}$ for USA, capturing both the higher values of the Eastern US and the lower values of the Western US. Its normalized mean error (NME) ranges from 40 to 60% being highest for the East Asia region, which also has the highest MB of $-1.65 \mu\text{g m}^{-3}$ (Table 3). Seasonally, the largest biases are found during summertime over Europe and the USA and during wintertime over East Asia (Table S4), while the same is true also for the predictions of ISORROPIA II in stable mode exhibiting quite similar metrics (Table S1). NH_4^+ is much better simulated by the model over the three regions, where the agreement with observations is high with MB values less than $0.4 \mu\text{g m}^{-3}$ but with slightly higher NME values (Table 4). Over Eastern Asia, the only important disparity is a slight underprediction of about $2 \mu\text{g m}^{-3}$ around Hong Kong following the underprediction of SO_4^{2-} over the same area (Fig. 3). Seasonally, spring is the worst period for the predictions of both versions, while there doesn't seem to be a consistent pattern of behavior for all three regions which perform best over different periods (Table S5 & S2). Finally, the model tends to overpredict NO_3^- concentrations over the three regions with MB values less than $1 \mu\text{g m}^{-3}$ albeit with high NME values (Table 5). Over East Asia, with the exception of Hong Kong, the model overestimates the NO_3^- concentrations by about $3 \mu\text{g m}^{-3}$, especially in the Wuhan and Guangzhou areas and also around Beijing (Fig. 3). In general, besides Hong Kong, the model overpredicts the concentrations of all three aerosol components examined here in the East Asian region. For all regions, the best seasonal agreement between the predictions of both versions in terms of MB values is found during the summer period, while the worst agreement occurs around the winter/spring period (Tables S6 & S3). The NME values are lowest in the summer for the USA and, surprisingly, in the winter for Europe and East Asia, even though this is the period with the worst MB values for these regions. Potential explanations include the coarse grid resolution used in this work as well as issues related to emissions (Zakoura and Pandis, 2018). It should be noted that even though the two versions perform similarly, better performance on certain statistical metrics should not be taken as an indication that one state assumption is more scientifically valid than the other. While a stable state could be considered more accurate under very low humidity conditions (e.g., over remote deserts; Karydis et al., 2016), in regions, such as those with intermediate RH and low nitrate concentration (e.g., Northeastern US), particles are mostly in metastable state (Guo et al., 2016). However, the two state assumptions produce very similar results in most cases, as shown here.

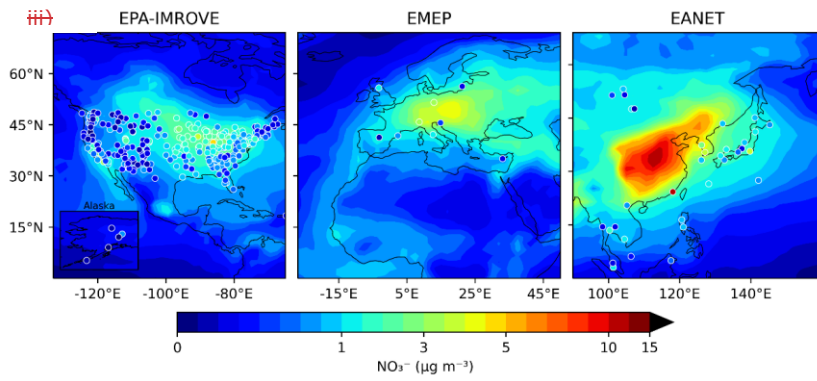
Annual mean SO_4^{2-} concentration (2010), modelled vs. observed



Annual mean NH_4^+ concentration (2010), modelled vs. observed



Annual mean NO_3^- concentration (2010), modelled vs. observed



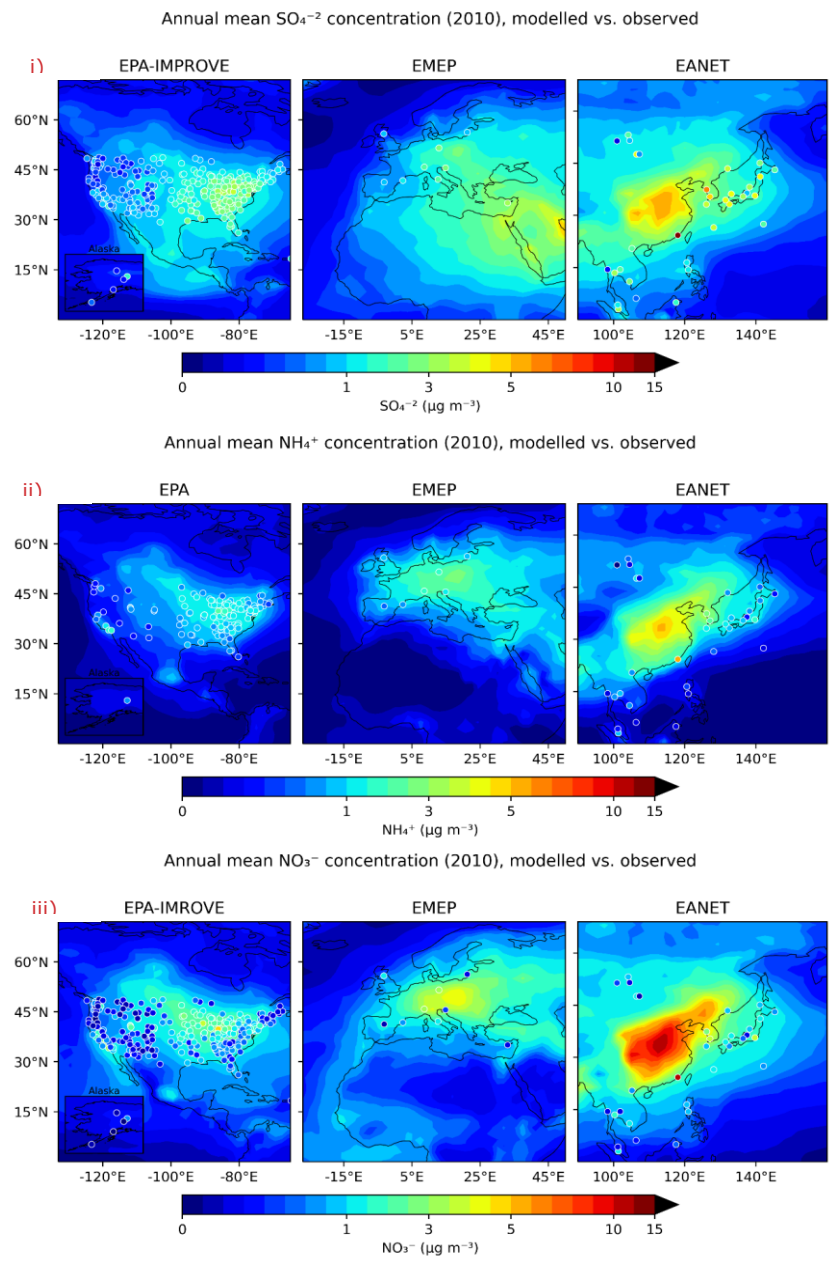


Figure 3: Annual mean surface concentrations of $\text{PM}_{2.5}$ i) SO_4^{2-} , ii) NH_4^+ , and iii) NO_3^- as simulated by EMAC using ISORROPIA-lite (shaded contours) versus observations of the same species from the IMPROVE, EMEP and EANET networks (colored circles).

Formatted: Font: 11 pt, Underline, Font color: Auto

Table 3: Statistical evaluation of EMAC predicted surface concentrations of $\text{PM}_{2.5} \text{SO}_4^{2-}$ using ISORROPIA-lite against observations during 2010.

Network	Number of datasets	Mean Observed ($\mu\text{g m}^{-3}$)	Mean Predicted ($\mu\text{g m}^{-3}$)	MAGE ($\mu\text{g m}^{-3}$)	MB ($\mu\text{g m}^{-3}$)	NME (%)	NMB (%)	RMSE ($\mu\text{g m}^{-3}$)
EPA	1791	2.18	1.28	0.92	-0.90	42	-38	0.93
IMPROVE	1526	1.02	0.92	0.47	-0.10	46	-11	0.73
EMEP	108	1.71	1.27	0.75	-0.44	44	-26	0.91
EANET	353	3.19	1.54	1.95	-1.65	61	-51	2.46

Table 4: Statistical evaluation of EMAC predicted surface concentrations of $\text{PM}_{2.5} \text{NH}_4^+$ using ISORROPIA-lite against observations during 2010.

Network	Number of datasets	Mean Observed ($\mu\text{g m}^{-3}$)	Mean Predicted ($\mu\text{g m}^{-3}$)	MAGE ($\mu\text{g m}^{-3}$)	MB ($\mu\text{g m}^{-3}$)	NME (%)	NMB (%)	RMSE ($\mu\text{g m}^{-3}$)
EPA	1660	1.01	1.01	0.50	0.00	49	0	0.72
IMPROVE	-	-	-	-	-	-	-	-
EMEP	84	1.08	1.44	0.63	0.36	59	34	0.75
EANET	360	0.93	1.25	0.69	0.32	74	34	1.25

Table 5: Statistical evaluation of EMAC predicted surface concentrations of $\text{PM}_{2.5} \text{NO}_3^-$ using ISORROPIA-lite against observations during 2010.

Network	Number of datasets	Mean Observed ($\mu\text{g m}^{-3}$)	Mean Predicted ($\mu\text{g m}^{-3}$)	MAGE ($\mu\text{g m}^{-3}$)	MB ($\mu\text{g m}^{-3}$)	NME (%)	NMB (%)	RMSE ($\mu\text{g m}^{-3}$)
EPA	1762	1.39	1.87	1.06	0.48	76	42	1.65
IMPROVE	1526	0.42	1.18	0.82	0.76	194	175	1.15
EMEP	108	1.15	1.91	1.25	0.76	109	66	1.66
EANET	372	1.32	2.27	1.33	0.95	101	72	2.17

3.4 Computational speed-up metrics

The computational efficiency and speed-up that ISORROPIA-lite provides compared to ISORROPIA II in both stable and metastable modes were quantified. Table 6 contains the total number of time steps that the EMAC model performed for the same simulation period (i.e., 24 h of CPU-time using 16 nodes) as well as the real time that was needed per individual time step, for each ISORROPIA version. The metrics shown in Table 6 concern the average value of each quantity, along with the corresponding standard deviation, resulting from a total of 18 simulations (6 for each version). From the difference in the real time required by the model to execute each individual time step, the speed-up of ISORROPIA-lite was found to be ~~close to 4~~ just above 3% compared to ISORROPIA II in metastable mode and ~~more than almost~~ 5 % compared to ISORROPIA II in stable mode. These values are, as expected, lower than the improvement in the computational efficiency that the ISORROPIA-lite version provides compared to the original version, as found in the offline evaluation, because EMAC contains several other modules that are quite computationally expensive. For example, the gas-phase chemistry (MECCA submodel) as well as wet deposition and liquid phase chemistry (SCAV submodel) are responsible for two thirds of the total computational cost of the global model. As a comparison, the offline speed-up that ISORROPIA-lite provided was calculated to be 35% and when utilized in the regional model PMCAMx 3D it was found to be 10% (Kakavas et al., 2022).

Table 6: Total number of time steps that EMAC executed in 24 hours of running time and number of seconds needed for each time step, utilizing ISORROPIA-lite and ISORROPIA II (both in Stable & Metastable). The computational speed-up refers to how much quicker (in %) the process is executed by ISORROPIA-lite in comparison to the previous version in both modes.

Simulation	# Time Steps	# Seconds per Timestep	Computational Speed-Up (%)
ISORROPIA-lite	78,074,193 ± 116	1.10 ± 0.002	-
ISORROPIA II v2.3 (Metastable)	75,403,720 ± 242	1.14 ± 0.003	3.73 ± 0.3
ISORROPIA II v2.3 (Stable)	74,429,599 ± 169	1.16 ± 0.003	5.54.8 ± 0.3

Formatted Table

4. Comparison of ISORROPIA-lite Against ISORROPIA II in Stable Mode

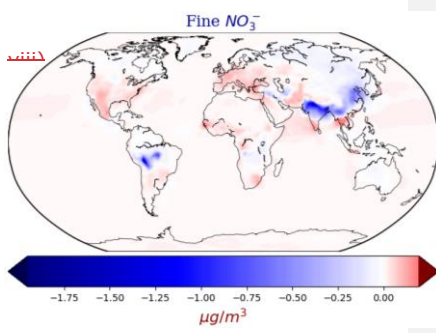
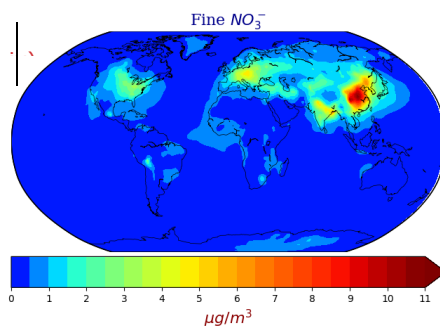
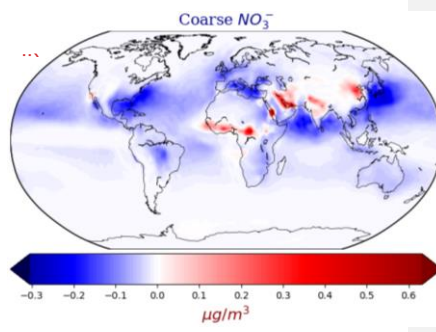
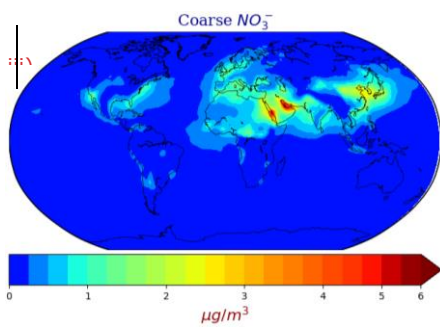
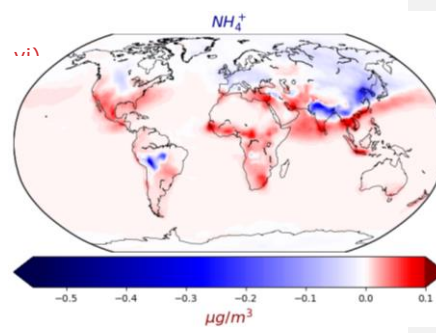
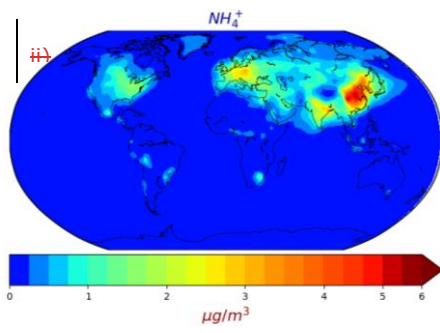
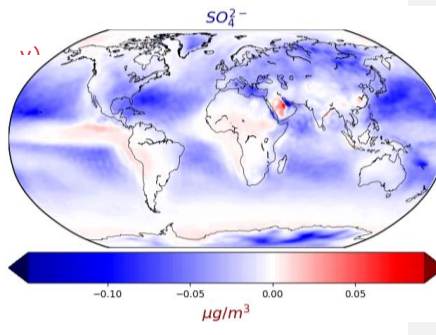
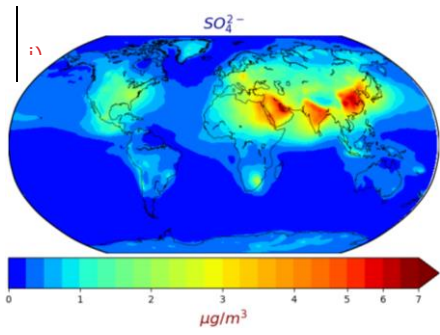
In this section, we present a comparison of the ISORROPIA-lite results in metastable mode against those of the ISORROPIA II results in stable mode. Both versions are now available in the latest version of the EMAC model, and the user has the option to utilize either one. While ISORROPIA-lite always assumes metastable aerosols, ISORROPIA II assumes stable aerosols by default. This comparison is done in an attempt to quantify the effects of using the metastable case in global atmospheric simulations, and to identify the regions and conditions under which the two assumptions have any significant, ~~but otherwise expected differences.~~ ~~We also investigate differences in the calculated aerosol acidity by the two modules.~~ differences. Some discrepancies are expected due to the different physical state of aerosols at low RH, however, the choice between a stable state and a metastable state should not be considered obvious. For example, Fountoukis et al. (2009) and Karydis et al. (2010) have shown that the stable assumption is in better agreement with observations under conditions where RH is consistently below 50%. On the other hand, Ansari and Pandis (2000) emphasize that the metastable assumption must be considered for regions characterized by intermediate RH and low pollutant concentrations (in this case of NO_3^-), while there are no significant differences between the two assumptions over regions with high concentrations. Here, differences in the calculated aerosol acidity by the two modules are also investigated.

4.1 Spatial variability of mean annual aerosol concentrations

For sulfate in TSP the predicted maximum annual average concentration was $7 \mu\text{g m}^{-3}$ found over East Asia highlighting the large anthropogenic impact over that region, while it was also high ($> 5 \mu\text{g m}^{-3}$) in India, Europe, and the Middle East in both simulations (Fig. 4i). Absolute differences for sulfate in TSP were lower than $0.15 \mu\text{g m}^{-3}$ ($< 3\%$) and found mainly over the polluted northern hemisphere (mainly East USA & Europe) with slightly higher values simulated by ISORROPIA II (Fig. 4ii). This is most likely related to the also higher NO_3^- aerosol predictions by ISORROPIA-lite over the same regions (see below & Fig. 4viii). The higher SO_4^{2-} aerosol concentrations estimated by ISORROPIA II over the Middle East region are mainly due to changes in wet deposition induced by the different physical state of the aerosol due to the higher water content by ISORROPIA-lite. The simulated concentrations of NH_4^+ in TSP had maximum annual average values of $6 \mu\text{g m}^{-3}$ and were found mainly over East Asia, especially around the greater Beijing and Wuhan areas, while India and Europe also exhibited high mean annual values for TSP NH_4^+ ($> 3 \mu\text{g m}^{-3}$) (Fig. 4iii). The absolute differences for NH_4^+ in TSP between the two model versions are higher over the Himalayan and East Asian regions (in favor of ISORROPIA II) but apparently weaker over USA, the Middle East and Africa (ISORROPIA-lite predicts higher values), although never higher than $0.5 \mu\text{g m}^{-3}$ ($< 5\%$) (Fig. 4iv). Regarding aerosol NO_3^- concentrations in the coarse mode the maximum annual average of $6 \mu\text{g m}^{-3}$ was predicted at the Arabian Peninsula (Fig. 4v), while in the fine mode the maximum annual average value of $11 \mu\text{g m}^{-3}$ was predicted over the metropolitan areas of Wuhan and Guangzhou (Fig. 4vii). Other high annual average concentrations of fine aerosol NO_3^- are found in the Tibetan Plateau and most prominently in heavy industrial

regions such as East US, Eastern Asia and Europe (exceeding $4 \mu\text{g m}^{-3}$ in most of these areas) with the latter two regions contributing high annual average concentrations in the coarse mode as well. The absolute differences for coarse NO_3^- were similar in magnitude to those of NH_4^+ in TSP with the Middle East yielding higher values by ISORROPIA-lite while the opposite is true for Europe and East USA- (Fig. 4vi). The absolute differences for fine NO_3^- are higher than those for coarse NO_3^- reaching up to $1.75 \mu\text{g m}^{-3}$ mainly over the Tibetan Plateau ($\sim 30\%$) with ISORROPIA II predicting the higher values- (Fig. 4vii). Higher nitrate concentrations were also predicted by ISORROPIA II mainly close to the West coast of South America and North of Atacama Desert. Around those regions as well as the Tibetan Plateau, the relative humidity is often below 50% and 30% respectively (see Fig. 8) and the metastable assumption results in lower nitrate concentrations, in agreement with the findings of Ansari and Pandis (2000). At the same time, ISORROPIA II predicts a higher aerosol fraction for NO_3^- (up to 10%) for the West coast of South America and the Tibetan Plateau. This is not the case for East Asia (Fig. 5ii) although the low sulfate/nitrate ratio of that region, results to an excess of available NH_3 to react with HNO_3 and form ammonium nitrate that would justify the higher fine mode nitrate concentrations by the stable case of ISORROPIA II (Ansari and Pandis, 2000). A higher NO_3^- aerosol fraction (up to 10%) in the Middle East was exhibited by ISORROPIA-lite (Fig. 5ii). This area is characterized by increased mineral ion concentrations and high sulfate to nitrate ratios (Karydis et al., 2016) which led to higher coarse mode nitrate predictions by the metastable case (Ansari and Pandis, 2000), although the maximum difference was only $0.6 \mu\text{g m}^{-3}$ (Fig. 4vi, 4viii). The differences in coarse and fine NO_3^- among the two versions did not display any strong seasonality as they were only slightly higher during autumn (for East Asia) and winter (for India-Himalayas) (not shown). A comparison of the simulated aerosol concentrations at higher altitudes can be found in Figure S3, where the zonal mean annual average concentrations as well as their absolute differences between the two model versions are depicted. The deviations between the results of the two ISORROPIA versions are becoming smaller as the air masses move higher in the atmosphere, until they are practically identical at altitudes above 700hPa. Regarding the behavior of the mineral ions of Ca^{2+} , K^+ , and Mg^{2+} the majority of high concentrations are found around the largest desert regions of the Sahara, Gobi, Atacama and Namib deserts (Figure S3S4), with Ca^{2+} being evidently the most dominant across all minerals. Furthermore, the absolute difference maps (Fig. S3S4) show minimal differences in mean annual surface concentrations (mostly less than $0.5 \mu\text{g m}^{-3}$) between the simulations from the two model versions. This is also reflected in the comparison of zonal mean annual average concentrations and their differences, as shown in Figure S5.

In the heavily polluted regions (particularly East USA, Europe and East Asia), the particulate NO_3^- dominates compared to the gas phase HNO_3 (Fig. 5i). The fine-mode fraction of the particulate nitrate burden is bigger than the coarse-mode fraction over Eastern Asia, India, Europe, and Eastern USA, while in the large desert areas of the Middle East and the Sahara most of the particulate NO_3^- exists in the coarse mode (Fig. 5iii). The aerosol water fraction is low ($<30\%$) across the most arid regions of Sahara, Atacama, Namib and Gobi, while Europe has the highest continental average aerosol water content in the Northern Hemisphere polluted regions (Fig. 5v). ISORROPIA-lite predicts higher average aerosol water concentration globally since the particles cannot form solids, and the salts remain in a supersaturated metastable solution (Fig. 5vi).



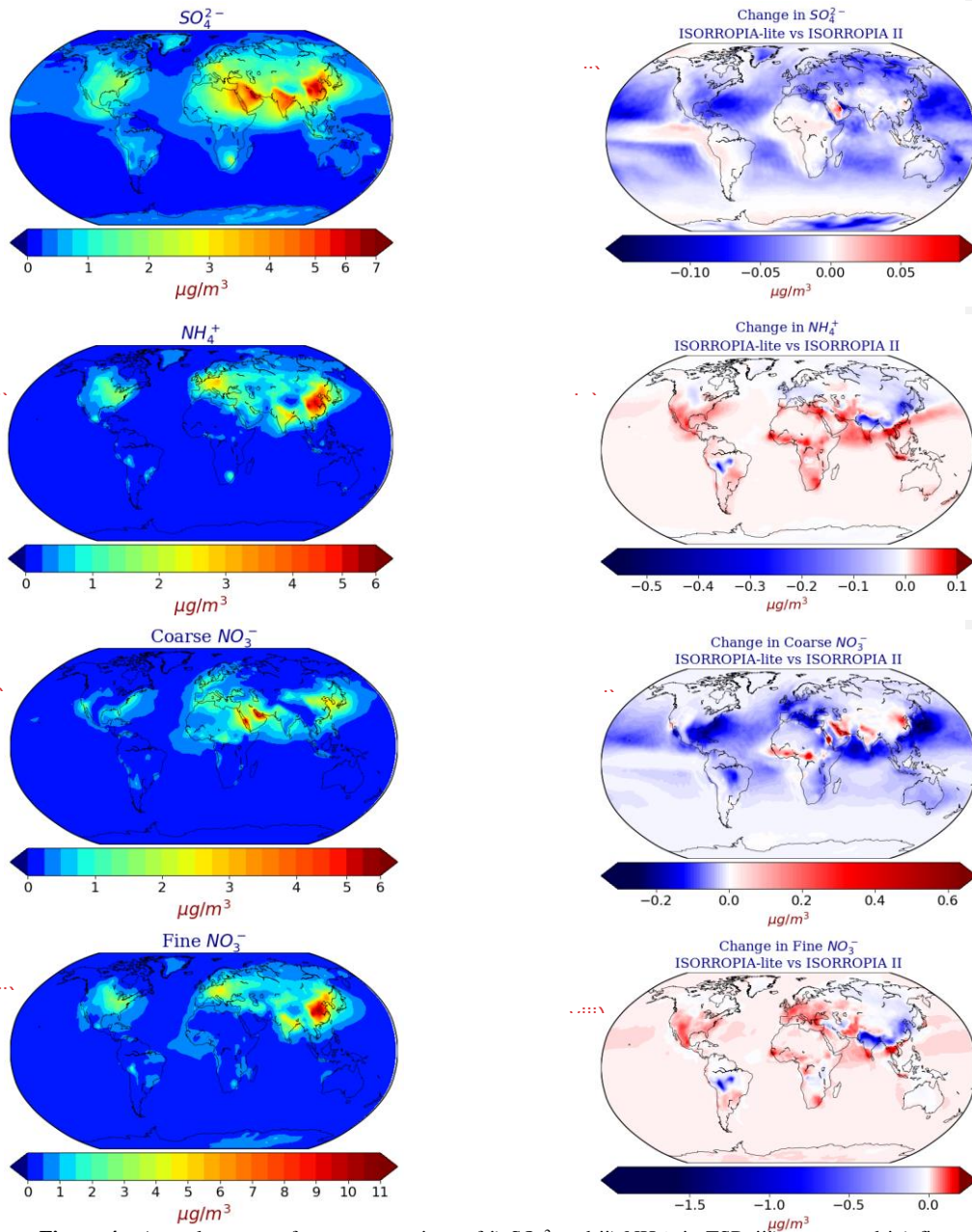
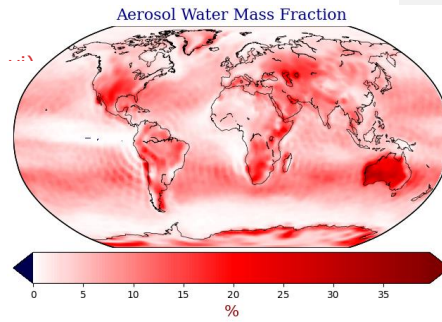
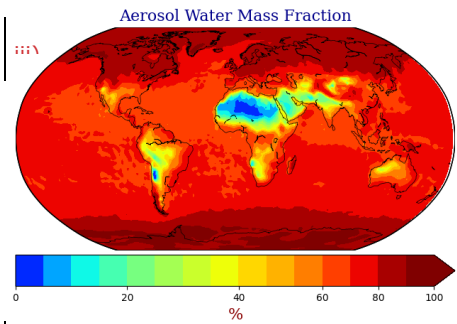
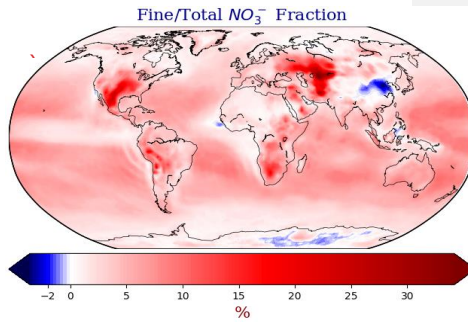
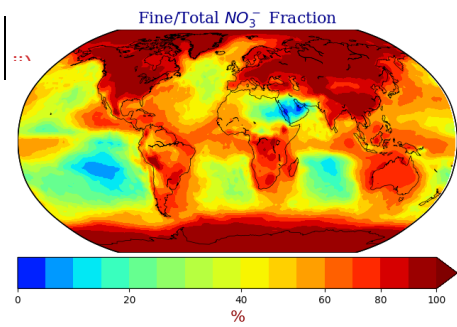
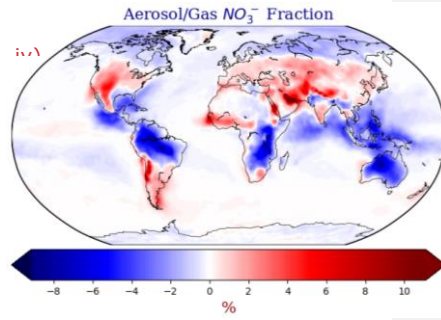
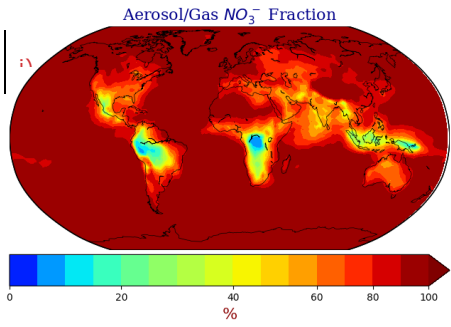


Figure 4 : Annual mean surface concentrations of i) SO_4^{2-} and ii) NH_4^+ in TSP, iii) coarse and iv) fine aerosol NO_3^- as predicted by EMAC using ISORROPIA-lite. Change of the annual mean EMAC-simulated surface concentration of v) NH_4^+ and vi) SO_4^{2-} in TSP, vii) coarse and viii) fine aerosol NO_3^- after employing ISORROPIA II. Positive values in red indicate higher concentrations by ISORROPIA-lite. The models assume different aerosol states.



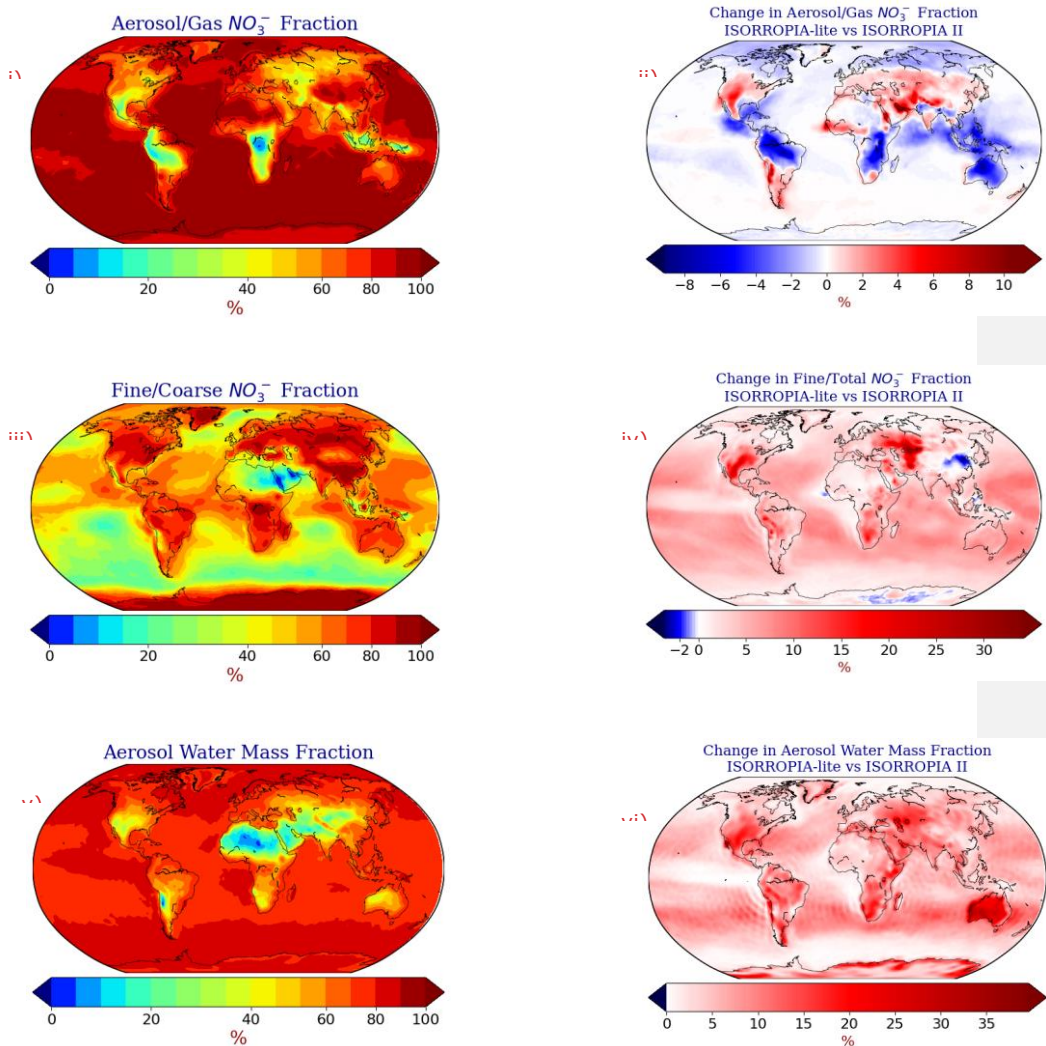
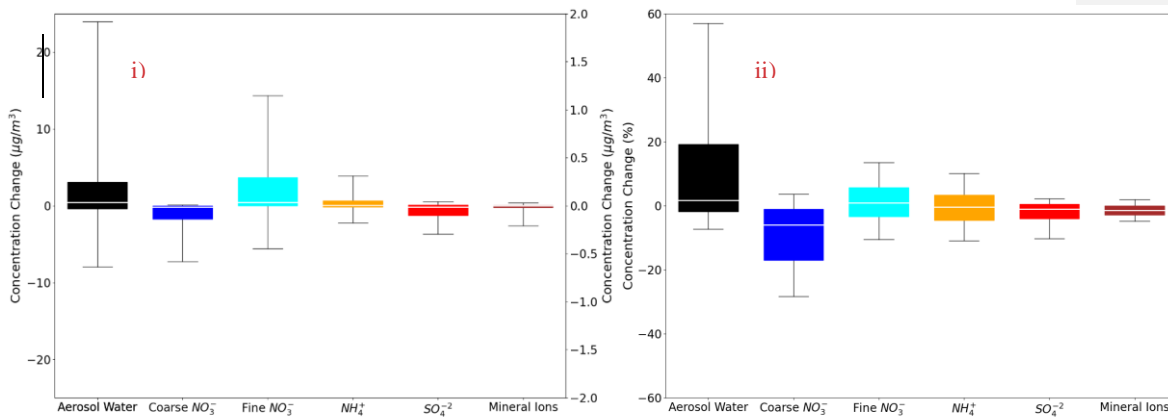
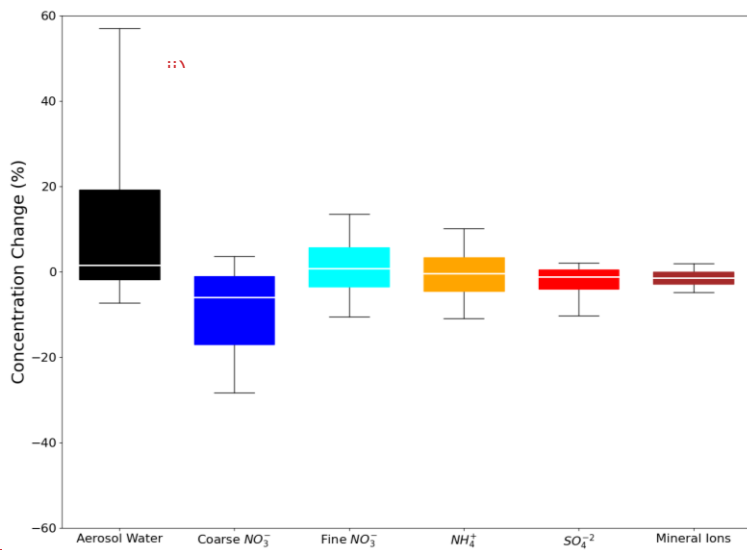
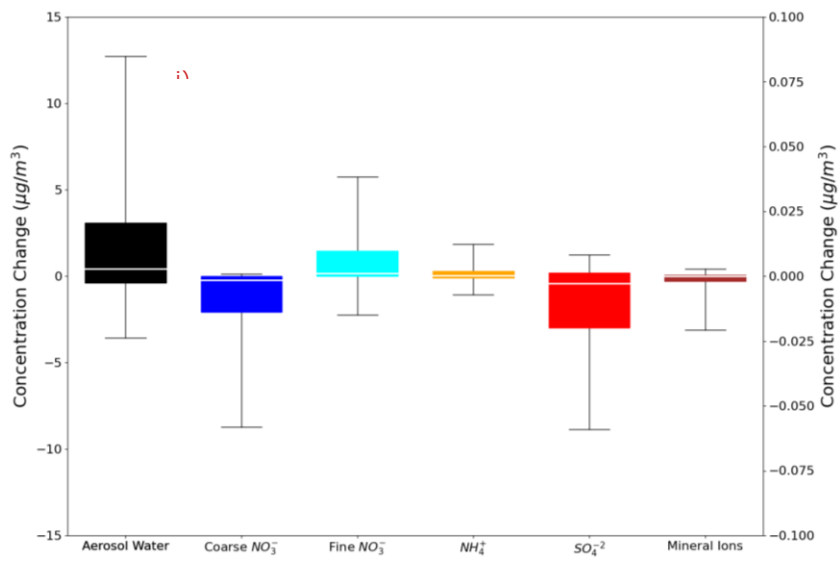


Figure 5 : Annual mean surface fractions of i) aerosol/gas NO_3^- , ii) fine/total-aerosol NO_3^- and iii) aerosol water mass as calculated by EMAC using ISORROPIA-lite. Change of the annual mean EMAC-simulated surface fractions of aerosol/gas iv) NO_3^- , v) fine/total-aerosol NO_3^- , and vi) aerosol water mass after employing ISORROPIA II. Positive values in red indicate higher fractions by ISORROPIA-lite. The models assume different aerosol states.

The absolute differences in global daily mean concentrations are mostly less than 0.0253 $\mu\text{g m}^{-3}$ (with differences for the 10th and 90th percentiles up to 0.075 $\mu\text{g m}^{-3}$) for all species (NH_4^+ , SO_4^{2-} and Mineral Cations in TSP as well as coarse and fine aerosol NO_3^-) except aerosol water in TSP (Figure 6). In that case the absolute differences for the 25th and 75th percentiles are less than 45 $\mu\text{g m}^{-3}$ (with differences for the 10th and 90th percentiles up to 13 $\mu\text{g m}^{-3}$). This translates to fractional differences for the 25th and 75th percentiles mostly below 20 % (and up to 60 % for differences in the 10th and 90th percentiles) for aerosol water in TSP and coarse NO_3^- aerosol, and mostly below 10 % for differences in the 25th and 75th percentiles (and up to 15 % for differences in the 10th and 90th percentiles) 5% for all the remaining species.





Formatted: Font: 11 pt, Bold, Underline

Figure 6 : Bar chart plots depicting the 25th, 50th and 75th percentiles (box) of the i) difference and ii) fractional difference in global daily mean surface concentrations of aerosol water (left y-axis), mineral ions, NH_4^+ and SO_4^{2-} in TSP as well as coarse and fine aerosol NO_3^- (right y-axis), as predicted by EMAC using ISORROPIA-lite and ISORROPIA II. The models assume different aerosol states at low RH and a positive change corresponds to higher concentrations by ISORROPIA-lite.

Formatted: Font: 11 pt, Font color: Auto

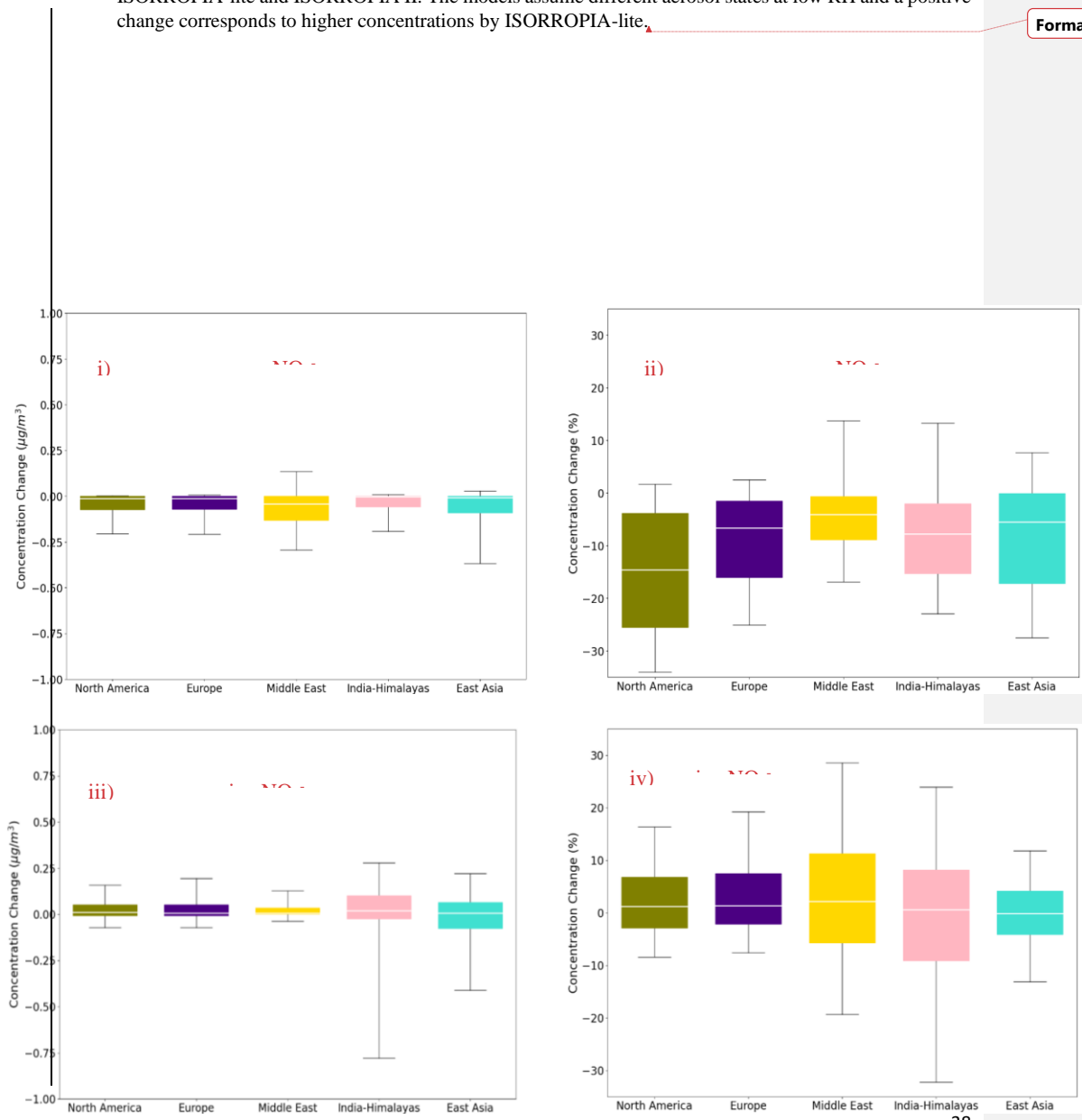
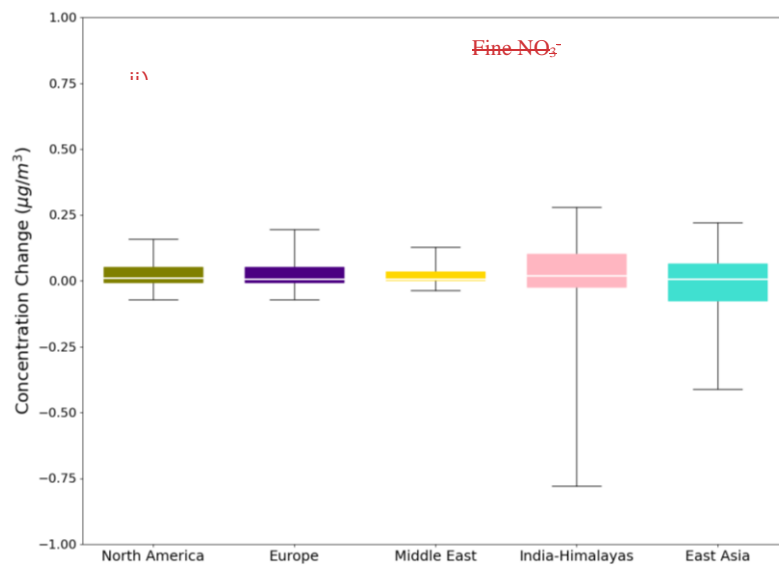
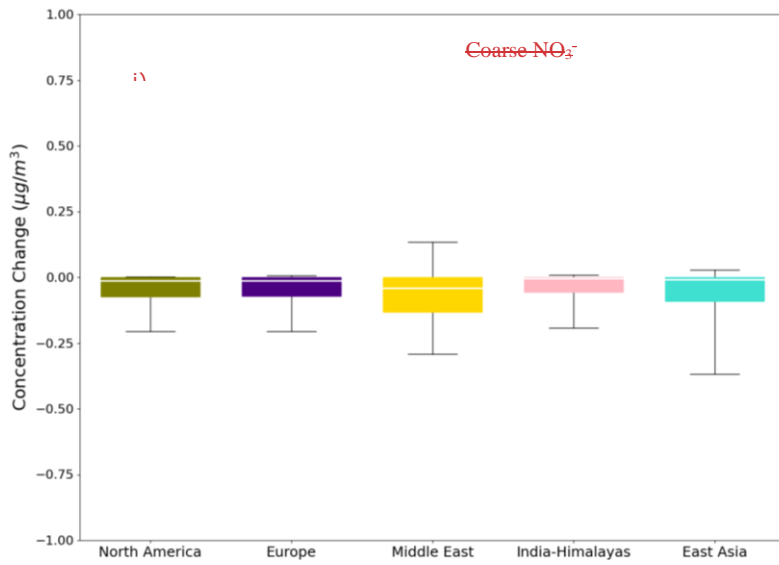
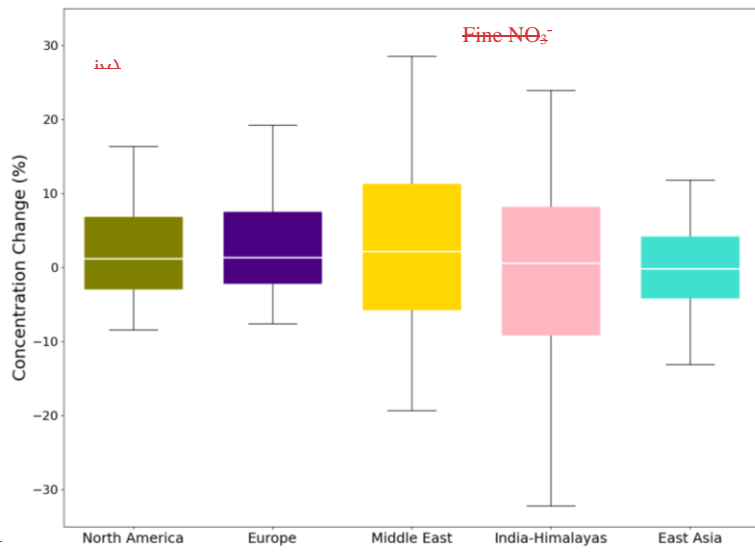
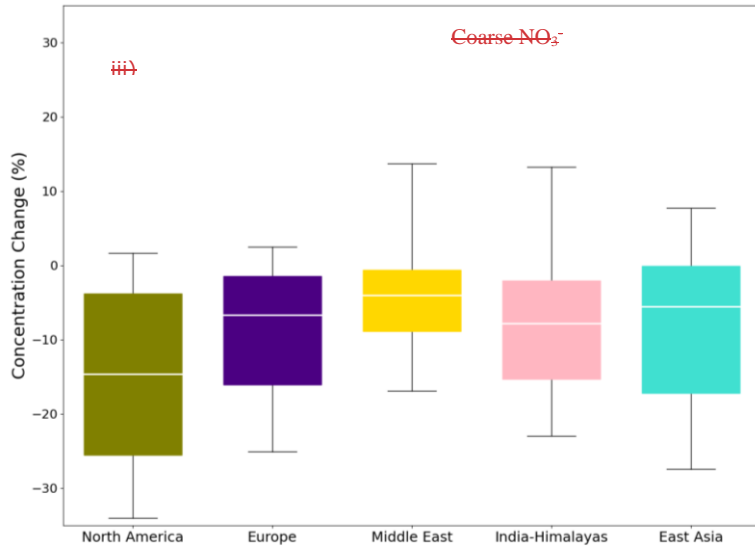


Figure 7: Bar chart plots depicting the 25th, 50th and 75th percentiles (box) of the difference in the global daily mean surface concentrations of i) coarse and ii) fine aerosol NO₃⁻ for the regions of North America, Europe, Middle East, India-Himalayas and East Asia, as predicted by EMAC using ISORROPIA-lite and ISORROPIA II. The fractional differences in global daily mean surface concentrations of iii) coarse and iv) fine aerosol NO₃⁻ for the same regions are also shown. The models assume different aerosol states at low RH and a positive change corresponds to higher concentrations by ISORROPIA-lite.-

The model results in the regions with the highest mean annual ~~load for the loads of~~ fine and coarse aerosol NO₃⁻ concentrations (see ~~section 3.1~~Section 3.1) as well as the most significant differences in estimated aerosol water and aerosol acidity (see Section 4.3), were further analyzed to determine whether the phase state assumption has a large ~~impaceteffect~~ on ~~the~~ simulated aerosol nitrate formation (Figure 7). For both coarse and fine daily mean NO₃⁻ concentrations, Europe and North America are clearly the regions with the smallest differences between the two versions. On the other hand, East Asia and especially the India-Himalayas regions are areas where the differences are the highest with ISORROPIA II predicting higher fine aerosol NO₃⁻ concentrations while in the Middle East, ISORROPIA-lite is predicting higher coarse mode aerosol NO₃⁻ concentrations. However, even for these areas the differences are typically below 0.25 µg m⁻³ (25th and 75th percentiles) with the higher differences not exceeding 0.8 µg m⁻³ (10th and 90th percentiles). This translates to fractional differences below 25 % (25th and 75th percentiles) for all regions, reaching up to 30 % (10th and 90th percentiles) mainly in the Tibetan Plateau and the Middle East.





Formatted: Font color: Auto

~~Figure 7. Bar chart plots depicting the 25th, 50th and 75th percentiles (box) of the difference in the global daily mean surface concentrations of i) coarse and ii) fine aerosol NO₃⁻ for the regions of North America, Europe, Middle East, India Himalayas and East Asia, as predicted by EMAC using ISORROPIA-lite and ISORROPIA-II. The fractional differences in global daily mean surface concentrations of iii) coarse and iv) fine aerosol NO₃⁻ for the same regions are also shown. The models assume different aerosol states at low RH and a positive change corresponds to higher concentrations by ISORROPIA-lite.~~

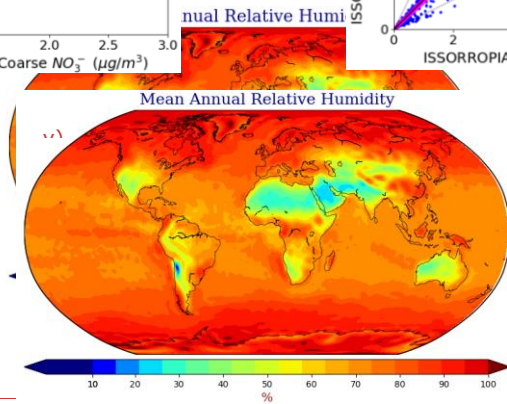
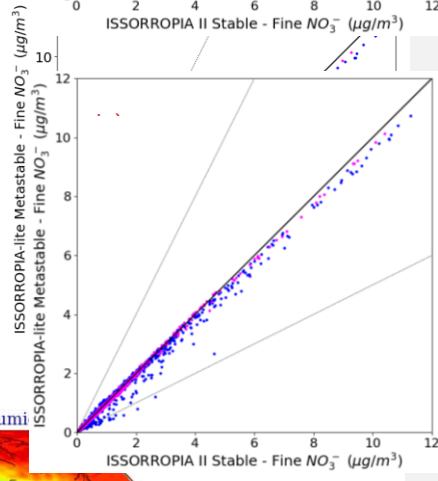
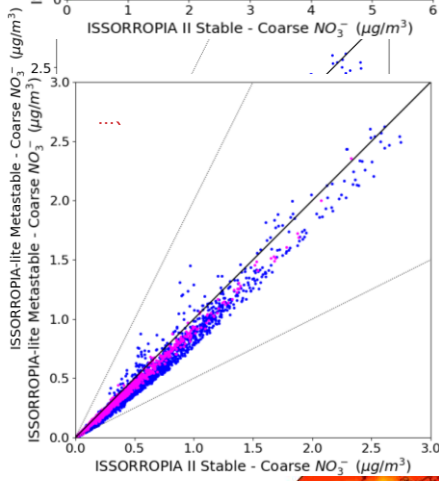
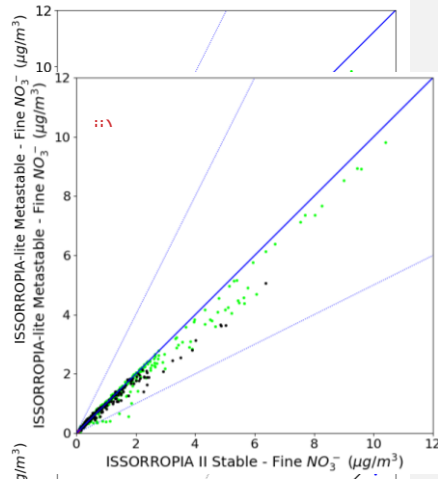
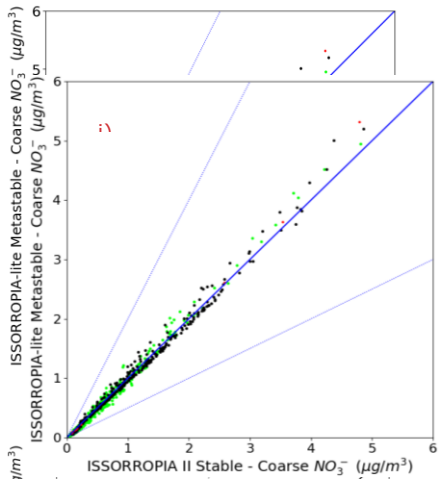
Table 7 contains the statistics for the comparisons of the global daily average surface concentrations calculated by the two simulations. While all the aerosol component concentrations, except for aerosol water, are higher for ISORROPIA II, the differences are still quite low. Furthermore, despite the different aerosol phase state assumption by the two versions, the normalized mean absolute difference remains low for all species (on average < ~~10~~11 %) except HNO₃. The overall statistics support the conclusion that on the global scale, the phase state assumption for low RH does not have a significant impact on the predicted tropospheric aerosol load. More specifically, ISORROPIA-lite produces a slightly higher tropospheric burden for aerosol NO₃⁻ than ISORROPIA II (0.875 Tg versus 0.861 Tg, respectively) while the opposite was the case for HNO₃ (0.921 Tg versus 0.935 Tg). The higher burden of ISORROPIA-lite is due to the fact that the higher aerosol water content favors the partitioning of HNO₃ to the particulate phase.

Table 7: Statistical analysis of EMAC-simulated mean ~~annual~~daily surface concentrations by employing ISORROPIA-lite in **metastable mode** versus ISORROPIA II in **stable mode**.
Bias is given as ISORROPIA₋lite – ISORROPIA II.

	Mean Difference ($\mu\text{g}/\text{m}^3$)	Normalized Mean Absolute Difference (%)
Coarse NO_3^-	-0.03 <u>0.26</u>	6.2
Fine NO_3^-	-0.02 <u>5.044</u>	7.6
HNO_3	-0.01 <u>2.002</u>	12.6
NH_4^+	-1.8 $\times 10^{-4}$	69.1
SO_4^{2-}	-0.00 <u>4.020</u>	9.8
Na^+	-0.01 <u>2.081</u>	10.3
Ca^{2+}	-0.06 <u>6.005</u>	38.0
K^+	-0.01 <u>1.002</u>	4.8
Mg^+	-0.00 <u>6.002</u>	8.6 <u>0</u>
Cl^-	-0.01 <u>2.120</u>	2.0
H_2O	-0.095	2.2
H^+	-1.320	3.0
pH Accumulation	-6 $\times 10^{-2}$ <u>7.17</u>	1.7
pH Coarse	-4.7 $\times 10^{-4}$	1.8
	-0.06 (pH)	1.7
	0.03 (pH)	9.4
		10.8
		6.6 <u>1</u>
		3.6
		5.5
		2.3
		2.3

4.2 Relative humidity dependent behavior of NO_3^- aerosols

The dependence of the differences in nitrate predictions on relative humidity was examined both for fine and coarse particles (Figure 8). The differences between ISORROPIA II and ISORROPIA-lite are higher at intermediate RH ranging from 20% to 60% being more evident in the fine mode aerosol NO_3^- and for high annual mean concentrations of coarse mode aerosol NO_3^- ($> 4 \mu\text{g m}^{-3}$). In this RH range, solid salts can precipitate when the stable equilibrium state is assumed (Seinfeld and Pandis, 2016), while in the metastable state all these salts remain dissolved in water. A region that has often RH in the 20 - 60% range is the Tibetan Plateau which leads to discrepancies of the fine mode particulate nitrate predictions of the two models in this area, while higher coarse mode particulate nitrate concentrations are predicted by ISORROPIA-lite in the Middle East, an area that is also often characterized by intermediate RH. The differences found for coarse mode particulate nitrate in the higher RH ranges of 60 – 100 %, can account for the respective differences that occurred in areas characterized by such RH values (East USA, Europe and East Asia) but concern lower annual mean concentration values ($< 3 \mu\text{g m}^{-3}$).



Formatted: Font: 11 pt, Bold, Underline

Formatted: Left, Indent: First line: 0 cm, Space After: 8 pt, Line spacing: Multiple 1.08 li

Figure 8: Scatterplots comparing the annual mean surface concentrations of coarse (i, iii) and fine aerosol NO_3^- (ii, iv) for relative humidity ranges of 20-60 % (i, ii) and 60-100 % (iii, iv) as predicted by EMAC using ISORROPIA-lite versus ISORROPIA II. The models assume different aerosol states at low RH. Black points represent the 20-40 % RH range, green points the 40-60 % range, blue points the 60-80 % range and pink points the 80-100 % range. v) Mean annual relative humidity as calculated by EMAC using ISORROPIA-lite.

4.3 Comparison of the estimated aerosol acidity

The estimated aerosol acidity by the two model versions was compared. separately for the accumulation and coarse size modes. This comparison aims at verifying the credibility of the estimated inorganic aerosol acidity of ISORROPIA-lite, as the first results of its implementation in the EMAC model are presented here. Since this capability is well established for ISORROPIA II (Karydis et al., 2021), it is of interest to examine any potential, but otherwise expected, differences between the two versions. The pH was computed for the fine and coarse particles, by:

$$\text{pH} = -\log_{10}\left(\frac{[\text{H}^+]}{[\text{H}_2\text{O}]}\right) \quad (1)$$

The calculations were performed neglecting the water associated with the organic fraction of aerosols, as they are handled by other parts of the aerosol microphysics submodel GMXe. The average pH was calculated based on the instantaneous H^+ and H_2O values estimated every 5 hours. This is because utilizing daily average values for H^+ and H_2O can result in a low-biased predicted pH of ~2 units globally (Karydis et al., 2021). The 5 hour interval provides a frequent output of values at different times of the day to account for the diurnal variability of pH, since a selection of 6 or 8 hour intervals would result in instantaneous H^+ and H_2O values at identical times on different days. pH calculations are performed only in cases where there is enough water in the aerosol (instantaneous values exceeding $0.05 \mu\text{g m}^{-3}$).

ISORROPIA-lite predicts slightly more acidic particles mainly in the coarse mode (Fig. 9iv). The most significant differences (up to 1 unit) in that size range are located over the Middle East and Arabian Peninsula, while smaller differences can be found in limited parts of the Himalayan and the East Asian regions as well as West USA and the Amazon Basin. These regions are characterized by high mineral cation concentrations and/or low RH. Therefore, the stable state results in increased pH values due to the precipitation of insoluble salts (e.g., CaSO_4) out of the aqueous phase. On the other hand, in the metastable state all anions remain in the aqueous phase lowering the particle pH. Differences in accumulation mode particle acidity are not as high (Fig. 9ii). ISORROPIA-lite predicts that accumulation mode particles over heavy industrialized regions such as Southeast Asia, Europe and Eastern USA are moderately acidic with mean pH values in the range of 4 - 5 while exhibiting alkaline behavior in desert areas where the increased levels of mineral ions elevate the pH above 7 (Fig. 9i). Coarse mode particles are in general more alkaline than those in the accumulation mode, with a few exceptions over east US, central Europe, north India and SE Asia (Fig. 9iii). These regions are characterized by high NH_3 concentrations from agricultural activities.

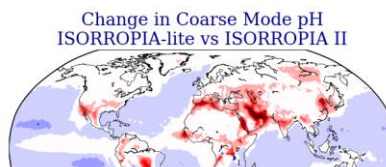
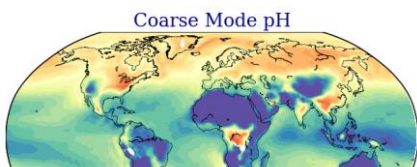
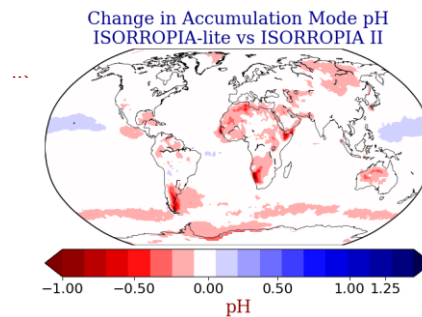
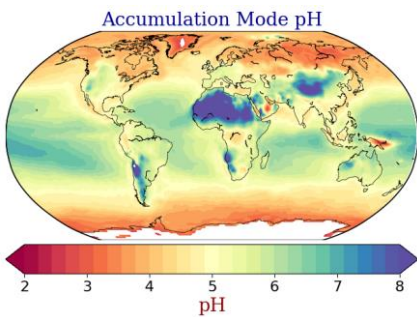
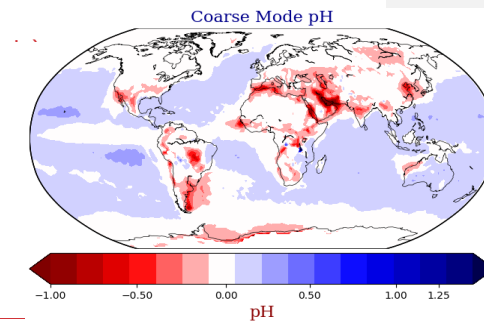
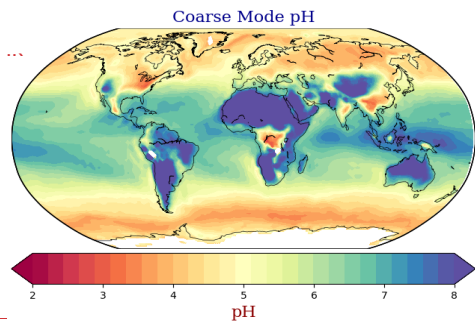
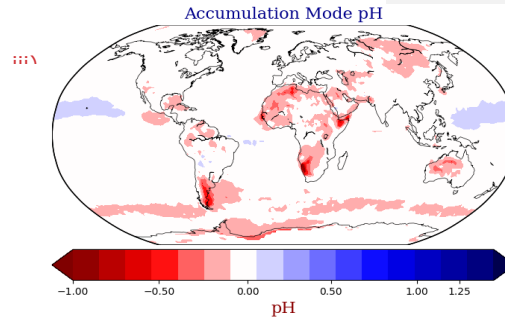
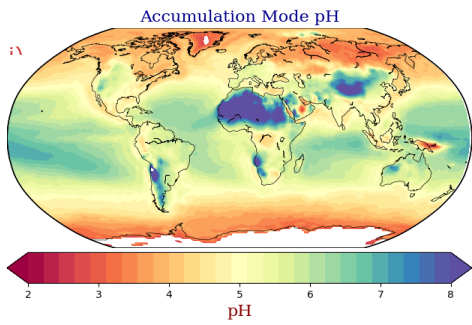


Figure 9: Annual mean EMAC-simulated i) accumulation and ii) coarse mode aerosol pH using ISORROPIA-lite. Change of the annual mean EMAC-simulated iii) accumulation and iv) coarse mode aerosol pH after using ISORROPIA II, with negative values in red indicating lower pH by ISORROPIA-lite. The models assume different aerosol states.

A sensitivity test was performed by ~~switching off~~ reducing all the NH_3 emissions ~~with the aim by half~~ to ~~deduce whether~~ investigate if there is a buffering mechanism that controls the pH of the accumulation mode particles more ~~strongly~~ than in the coarse mode. Figure 10 shows the difference of the mean annual calculated aerosol pH between the base case (NH_3 emissions present) and the sensitivity case (~~withou~~ half NH_3 emissions). When NH_3 emissions are switched off, the pH of fine PM decreases by up to 5.3 units and the particles become a lot more acidic (Fig. 10i). For the coarse mode this effect is not that strong (pH reduction of up to 2.1.5 units) (Fig. 10ii). As expected, this buffering mechanism is mainly observed across the aforementioned regions where NH_3 concentrations are high, but also over areas affected by natural NH_3 emissions. This is consistent with the results of Karydis et al. (2021) who found that in the absence of NH_3 , aerosol particles would be extremely acidic in most of the world.

The differences in the accumulation mode pH calculated by ISORROPIA-lite and ISORROPIA II are extremely small (i.e., mean difference of 0.06 pH units or 2.3%), and even smaller for coarse mode pH (Table 7), indicating an overall good agreement between the two model versions.

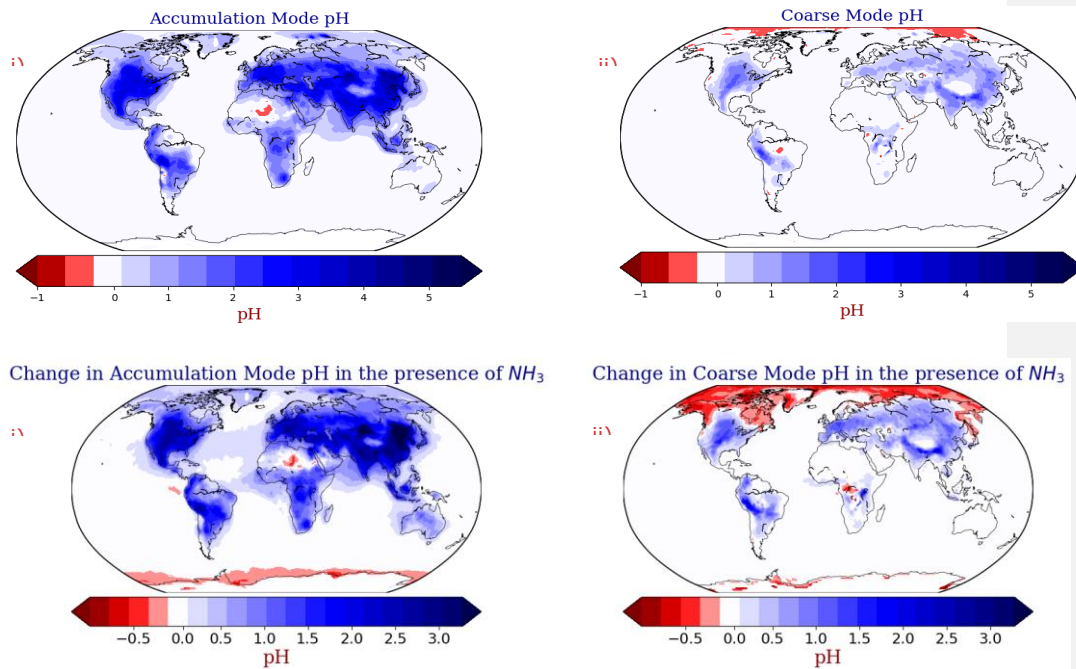


Figure 10: Absolute change of the annual mean EMAC-simulated i) accumulation and ii) coarse mode aerosol pH using ISORROPIA-lite after reducing switching off the NH_3 emissions by half. Positive values in blue indicate higher aerosol pH when NH_3 is present.

Formatted: Font: 11 pt, Bold, Underline
Formatted: Left, Indent: First line: 0 cm, Space After: 8 pt, Line spacing: Multiple 1.08 li

5. Conclusions

This study presents the first results of the implementation of the ISORROPIA-lite thermodynamic module in the EMAC global chemistry and climate model, and is compared to the previous version, ISORROPIA II v2.3, after the latter has successfully replaced ISORROPIA II v1 to improve pH predictions close to neutral conditions.

The results of ISORROPIA II versions 1 and 2.3 both in stable mode, had insignificant differences (<3%) concerning the global predictions of NH_4^+ , SO_4^{2-} , mineral ions and aerosol water in TSP concentrations as well as fine and coarse mode aerosol NO_3^- . The comparison of results from ISORROPIA-lite against ISORROPIA II v2.3 in metastable mode, showed also negligible differences (<5%) between all the examined aerosol components on a global scale. The comparison of the ISORROPIA-lite results for $\text{PM}_{2.5}$ NH_4^+ , SO_4^{2-} , and NO_3^- versus observations from the IMPROVE, EMEP and EANET networks reveals that East Asia is the area with the

largest discrepancies. There was satisfactory agreement in Europe and over the US for NH_4^+ and SO_4^{2-} , while ISORROPIA-lite predicted lower concentrations around Hong Kong with a maximum difference of $1.5 \mu\text{g m}^{-3}$ (~20 %) for these two species. For NO_3^- , the discrepancy was up to $3 \mu\text{g m}^{-3}$ (~30 %) in the same region, while a difference of about $1.5 \mu\text{g m}^{-3}$ (~25 %) was found over Central Europe with ISORROPIA-lite predicting the higher values. With the exception of Hong Kong, the model in general overpredicted the concentrations of all three aerosol components over the East Asian region.

A comparison between ISORROPIA-lite in the metastable state and ISORROPIA II in the stable state was performed to identify potential discrepancies ~~on in the EMAC-simulated~~ inorganic aerosol concentrations. ~~These simulated by EMAC. Although differences between the two model versions are to be expected due to the different physical state of aerosols at low RH, it is of interest to examine under which conditions these differences occur so that potential users are informed of the strengths and weaknesses of using either model version depending on the application. Both~~ modules are now ~~both~~ available as different options in the EMAC model. The agreement between the two versions was generally quite good for global daily mean surface concentrations of inorganic aerosols, mineral ions and aerosol water. More specifically mineral ions, SO_4^{2-} and NH_4^+ in TSP had the smallest differences overall, less than $0.5 \mu\text{g m}^{-3}$ even in localized extreme cases ~~and~~ but in the vast majority less than $0.051 \mu\text{g m}^{-3}$ (or less than 10.5%). For coarse NO_3^- aerosols the absolute differences were of similar magnitude with the higher concentrations simulated by ISORROPIA-lite in the Middle East being the most notable. In the case of fine NO_3^- aerosols, the differences were larger (up to $\sim 1.75 \mu\text{g m}^{-3}$ in local extremes), mainly over the West coast of South America (North of Atacama Desert), the Tibetan Plateau and Eastern Asia regions with higher concentrations simulated by ISORROPIA II but still within ~30%. In Europe and the US, the corresponding differences were less than $0.25 \mu\text{g m}^{-3}$. The most important difference was the higher aerosol water calculated by ISORROPIA-lite, especially for relative humidity in the 20% to 60 % range. However, this was less than $5 \mu\text{g m}^{-3}$ or 20 % in most cases. Therefore, even though local differences are expected in regions where the relative humidity is often in this range, on a global scale choosing a different physical state of the aerosol at lower RH does not have such a big impact.

When the relative humidity ranged from 20 % to 60 %, differences in coarse and fine NO_3^- concentrations predictions among the two versions increased. The highest discrepancies were found in the Tibetan Plateau and the Middle East regions both of which are dominated by such RH values during most of the year. In the first region, the combination of those RH values with mid-range temperatures does not favor nitrate aerosol formation if the aerosol is in the metastable state (ISORROPIA-lite). In the second region, the low RH values result in very low aerosol water predictions for the stable state assumed by ISORROPIA II which hinder the condensation of HNO_3 into the aerosol phase.

Investigation of the differences in the estimated inorganic aerosol acidity between the two versions, due to the different assumed aerosol phase states, is of great interest for potential future use of ISORROPIA-lite in global climate simulations. ISORROPIA-lite produces slightly more acidic coarse mode aerosols (in comparison to ISORROPIA II) but by less than 1 pH unit on average. The most important differences were found mainly in the Middle East and Arabian Peninsula due to the presence of high mineral cation concentrations. The stable state considered

by ISORROPIA II allows the precipitation of insoluble salts and removes anions from the aqueous phase that would otherwise deplete the pH, while this is not the case for the metastable aerosol state considered by ISORROPIA-lite. Furthermore, NH_3 is found to control the aerosol acidity of both fine and coarse mode particles, however, it provides significantly larger buffering capacity to the accumulation mode than to the coarse. This results in slightly more basic accumulation particles than coarse in regions with high NH_3 presence from agricultural activities and low mineral cation concentrations (e.g., Europe).

Finally concerning the computational efficiency that ISORROPIA-lite provides when used by the EMAC global model, a speed-up of ~~more than 3~~close to 4% was achieved compared to ISORROPIA II in metastable state and ~~nearly more than~~ 5% compared to ISORROPIA-II in stable state.

Code and Data Availability

The usage of MESSy (Modular Earth Submodel System) and access to the source code is licensed to all affiliates of institutions which are members of the MESSy Consortium. Institutions can become a member of the MESSy Consortium by signing the MESSy Memorandum of Understanding. More information can be found on the MESSy Consortium Website <http://www.messy-interface.org>. The code ~~used~~developed in this study ~~is available from and all relevant features, including~~ the ~~author upon request~~. ~~The ISORROPIA II v2.3 and ISORROPIA-lite v1.0 thermodynamic equilibrium codes are available at <https://isorro피아.epfl.ch> as part of the MESSy system, are archived with a restricted access DOI (<https://doi.org/10.5281/zenodo.8379120>) and have already been incorporated into the official development branch of the EMAC modelling system and will therefore be part of all future released versions.~~ The data produced in the study are available from the author upon request.

Acknowledgements

This work was supported by the project FORCeS funded from the European Union's Horizon 2020 research and innovation program under grant agreement No 821205. The work described in this paper has received funding from the Initiative and Networking Fund of the Helmholtz Association through the project "Advanced Earth System Modelling Capacity (ESM)". The authors gratefully acknowledge the Earth System Modelling Project (ESM) for funding this work by providing computing time on the ESM partition of the supercomputer JUWELS (Alvarez, 2021) at the Jülich Supercomputing Centre (JSC).

Competing Interests

HT acts as a topical editor for GMD but has no further competing interests.

Author Contributions

AM and VAK wrote the paper with contributions from all coauthors. VAK planned the research with contributions from AKS, SNP and AN. AN and SNP provided the ISORROPIA-lite model. AM and HT performed the implementation in EMAC. AM performed the simulations and analyzed the results assisted by VAK and APT. APT provided the observations and performed the model evaluation. All the authors discussed the results and contributed to the manuscript.

References

- Alvarez, D.: JUWELS cluster and booster: Exascale pathfinder with modular supercomputing architecture at juelich supercomputing Centre. *Journal of large-scale research facilities JLSRF*, 7, A183-A183, <https://doi.org/10.17815/jlsrf-7-183>, 2021.
- Andreae, M. O., Jones, C. D., and Cox, P. M.: Strong present-day aerosol cooling implies a hot future. *Nature*, 435(7046), 1187-1190, <https://doi.org/10.1038/nature03671>, 2005.
- Ansari, A. S. and Pandis, S. N.: The effect of metastable equilibrium states on the partitioning of nitrate between the gas and aerosol phases. *Atmospheric Environment*, 34(1), 157-168, [https://doi.org/10.1016/S1352-2310\(99\)00242-3](https://doi.org/10.1016/S1352-2310(99)00242-3), 2000.
- Asthitha, M., Lelieveld, J., Abdel Kader, M., Pozzer, A., and De Meij, A: Parameterization of dust emissions in the global atmospheric chemistry-climate model EMAC: impact of nudging and soil properties. *Atmospheric Chemistry and Physics*, 12(22), 11057-11083, <https://doi.org/10.5194/acp-12-11057-2012>, 2012.
- Bacer, S., Sullivan, S. C., Karydis, V. A., Barahona, D., Kramer, M. and co-authors: Implementation of a comprehensive ice crystal formation parameterization for cirrus and mixed-phase clouds in the EMAC model (based on MESSy 2.53). *Geoscientific model development*, 11(10), 4021-4041, <https://doi.org/10.5194/gmd-11-4021-2018>, 2018.
- Bassett, M. and Seinfeld, J. H.: Atmospheric equilibrium model of sulfate and nitrate aerosols. *Atmospheric Environment (1967)*, 17(11), 2237-2252, [https://doi.org/10.1016/0004-6981\(83\)90221-4](https://doi.org/10.1016/0004-6981(83)90221-4), 1983.
- Bouwman, A. F., Lee, D. S., Asman, W. A., Dentener, F. J., Van Der Hoek, K. W., and Olivier, J. G. J.: A global high-resolution emission inventory for ammonia. *Global biogeochemical cycles*, 11(4), 561-587, <https://doi.org/10.1029/97GB02266>, 1997.
- Bromley, L. A.: Thermodynamic properties of strong electrolytes in aqueous solutions. *AIChE journal*, 19(2), 313-320, <https://doi.org/10.1002/aic.690190216>, 1973.
- Brook, R. D., Rajagopalan, S., Pope, C. A., Brook, J. R., Bhatnagar, A. and co-authors: Particulate matter air pollution and cardiovascular disease: an update to the scientific statement from the American Heart Association. *Circulation*, 121(21), 2331-2378, <https://doi.org/10.1161/CIR.0b013e3181d8ce1>, 2010.
- Chen, Y., Shen, H., and Russell, A. G.: Current and future responses of aerosol pH and composition in the US to declining SO₂ emissions and increasing NH₃ emissions. *Environmental Science & Technology*, 53(16), 9646-9655, <https://doi.org/10.1021/acs.est.9b02005>, 2019.
- Clegg, S. L., Seinfeld, J. H., and Edney, E. O.: Thermodynamic modelling of aqueous aerosols containing electrolytes and dissolved organic compounds. II. An extended Zdanovskii–Stokes–Robinson approach. *Journal of aerosol science*, 34(6), 667-690, [https://doi.org/10.1016/S0021-8502\(03\)00019-3](https://doi.org/10.1016/S0021-8502(03)00019-3), 2003.
- Crippa, M., Guizzardi, D., Muntean, M., Schaaf, E., Dentener, F. and co-authors: Gridded emissions of air pollutants for the period 1970–2012 within EDGAR v4. 3.2. *Earth Syst. Sci. Data*, 10(4), 1987-2013, <https://doi.org/10.5194/essd-10-1987-2018>, 2018.
- Dentener, F., Kinne, S., Bond, T., Boucher, O., Cofala, J. and co-authors: Emissions of primary aerosol and precursor gases in the years 2000 and 1750 prescribed data-sets for AeroCom. *Atmospheric Chemistry and Physics*, 6(12), 4321-4344, <https://doi.org/10.5194/acp-6-4321-2006>, 2006.
- Doney, S. C., Mahowald, N., Lima, I., Feely, R. A., Mackenzie, F. T., Lamarque, J. F., and Rasch, P. J.: Impact of anthropogenic atmospheric nitrogen and sulfur deposition on ocean acidification and the inorganic carbon system. *Proceedings of the National Academy of Sciences*, 104(37), 14580-14585, <https://doi.org/10.1073/pnas.0702218104>, 2007.
- EMEP Programme Air Pollutant Monitoring Data, available at : <https://projects.nilu.no/ccc/index.html>

- Fang, T., Guo, H., Zeng, L., Verma, V., Nenes, A., and Weber, R. J.: Highly acidic ambient particles, soluble metals, and oxidative potential: a link between sulfate and aerosol toxicity. *Environmental science & technology*, 51(5), 2611-2620, <https://doi.org/10.1021/acs.est.6b06151>, 2017.
- Fountoukis, C. and Nenes, A.: ISORROPIA II: a computationally efficient thermodynamic equilibrium model for K⁺–Ca²⁺–Mg²⁺–NH₄⁺–Na⁺–SO₄²⁻–NO₃⁻–Cl⁻–H₂O aerosols. *Atmospheric Chemistry and Physics*, 7(17), 4639-4659, <https://doi.org/10.5194/acp-7-4639-2007>, 2007.
- [Fountoukis, C., Nenes, A., Sullivan, A., Weber, R., Van Reken, T., Fischer, M., Matías, E., Moya, M., Farmer, D., and Cohen, R. C.: Thermodynamic characterization of Mexico City aerosol during MILAGRO 2006. *Atmospheric Chemistry and Physics*, 9\(6\), 2141-2156, <https://doi.org/10.5194/acp-9-2141-2009>, 2009.](#)
- Fu, X., Wang, S., Xing, J., Zhang, X., Wang, T., and Hao, J.: Increasing ammonia concentrations reduce the effectiveness of particle pollution control achieved via SO₂ and NO_x emissions reduction in east China. *Environmental Science & Technology Letters*, 4(6), 221-227, <https://doi.org/10.1021/acs.estlett.7b00143>, 2017.
- Grewe, V., Brunner, D., Dameris, M., Grenfell, J. L., Hein, R., Shindell, D., and Staehelin, J.: Origin and variability of upper tropospheric nitrogen oxides and ozone at northern mid-latitudes. *Atmospheric Environment*, 35(20), 3421-3433, [https://doi.org/10.1016/S1352-2310\(01\)00134-0](https://doi.org/10.1016/S1352-2310(01)00134-0), 2001.
- [Guo, H., Sullivan, A. P., Campuzano-Jost, P., Schroder, J. C., Lopez-Hilfiker, F. D., Dibb, J. E., Jimenez, J. L., Thornton, J. A., Brown, S. S., Nenes, A., and Weber, R. J.: Fine particle pH and the partitioning of nitric acid during winter in the northeastern United States. *Journal of Geophysical Research: Atmospheres*, 121, 10, 355-310, 376, <https://doi.org/10.1002/2016JD025311>, 2016.](#)
- He, K., Yang, F., Ma, Y., Zhang, Q., Yao, X., Chan, C. K., Cadle, S., Chan, T., and Mulawa, P.: The characteristics of PM_{2.5} in Beijing, China, *Atmospheric Environment*, 35(29), 4959-4970, [https://doi.org/10.1016/S1352-2310\(01\)00301-6](https://doi.org/10.1016/S1352-2310(01)00301-6), 2001.
- Héroux, M. E., Anderson, H. R., Atkinson, R., Brunekreef, B., Cohen, A., Forastiere, F. and co-authors: Quantifying the health impacts of ambient air pollutants: recommendations of a WHO/Europe project. *International journal of public health*, 60, 619-627, <https://doi.org/10.1007/s00038-015-0690-y>, 2015.
- Hersbach, H., Bell, B., Berrisford, P., Hirahara, S., Horanyi, A. and co-authors: The ERA5 global reanalysis. *Quarterly Journal of the Royal Meteorological Society*, 146(730), 1999-2049, <https://doi.org/10.1002/qj.3803>, 2020.
- Honour, S. L., Bell, J. N. B., Ashenden, T. W., Cape, J. N., and Power, S. A.: Responses of herbaceous plants to urban air pollution: effects on growth, phenology and leaf surface characteristics. *Environmental pollution*, 157(4), 1279-1286, <https://doi.org/10.1016/j.envpol.2008.11.049>, 2009.
- Interagency Monitoring of Protected Visual Environment (IMPROVE), available at : <http://vista.cira.colostate.edu/Improve/improve-data/>
- Jacobson, M. Z., Tabazadeh, A., and Turco, R. P.: Simulating equilibrium within aerosols and nonequilibrium between gases and aerosols. *Journal of Geophysical Research: Atmospheres*, 101(D4), 9079-9091, <https://doi.org/10.1029/96JD00348>, 1996.
- Jöckel, P., Sander, R., Kerkweg, A., Tost, H., and Lelieveld, J.: the modular earth submodel system (MESSy)- a new approach towards earth system modeling. *Atmospheric Chemistry and Physics*, 5(2), 433-444, <https://doi.org/10.5194/acp-5-433-2005>, 2005.
- Jockel, P., Tost, H., Pozzer, A., Bruhl, C., Buchholz, J. and co-authors: The atmospheric chemistry general circulation model ECHAM5/MESSy1: consistent simulation of ozone from the surface to the mesosphere. *Atmospheric Chemistry and Physics*, 6(12), 5067-5104, <https://doi.org/10.5194/acp-6-5067-2006>, 2006.

- Jockel, P., Tost, H., Pozzer, A., Kunze, M., Kirner, O. and co-authors: Earth system chemistry integrated modelling (ESCI-Mo) with the modular earth submodel system (MESSy) version 2.51. *Geoscientific Model Development*, 9(3), 1153-1200, <https://doi.org/10.5194/gmd-9-1153-2016>, 2016.
- Kakavas, S., Pandis, S. N., and Nenes, A.: ISORROPIA-Lite: A Comprehensive Atmospheric Aerosol Thermodynamics Module for Earth System Models. *Tellus B: Chemical and Physical Meteorology*, 74(2022), <https://doi.org/10.16993/tellusb.33>, 2022.
- Kakavas, S., Pandis, S., and Nenes, A.: Effects of Secondary Organic Aerosol Water on fine PM levels and composition over US. *Atmospheric Chemistry and Physics [preprint]*, <https://doi.org/10.5194/acp-2022-815>, 16 January 2023.
- Karydis, V. A., Tsimpidi, A. P., Fountoukis, C., Nenes, A., Zavala, M., Lei, W. F., Molina, L. T., and Pandis, S. N.: Simulating the fine and coarse inorganic particulate matter concentrations in a polluted megacity, *Atmospheric Environment*, 44(5), 608-620, <https://doi.org/10.1016/j.atmosenv.2009.11.023>, 2010.
- Karydis, V. A., Tsimpidi, A. P., Lei, W., Molina, L. T., and Pandis, S. N.: Formation of semivolatile inorganic aerosols in the Mexico City Metropolitan Area during the MILAGRO campaign. *Atmospheric Chemistry and Physics*, 11(24), 13305-13323, <https://doi.org/10.5194/acp-11-13305-2011>, 2011.
- Karydis, V. A., Tsimpidi, A. P., Pozzer, A., Astitha, M., and Lelieveld, J.: Effects of mineral dust on global atmospheric nitrate concentrations. *Atmospheric Chemistry and Physics*, 16(3), 1491-1509, <https://doi.org/10.5194/acp-16-1491-2016>, 2016.
- Karydis, V. A., Tsimpidi, A. P., Bacer, S., Pozzer, A., Nenes, A., and Lelieveld, J.: Global impact of mineral dust on cloud droplet number concentration. *Atmospheric Chemistry and Physics*, 17(9), 5601-5621, <https://doi.org/10.5194/acp-17-5601-2017>, 2017.
- Karydis, V. A., Tsimpidi, A. P., Pozzer, A., and Lelieveld, J.: How alkaline compounds control atmospheric aerosol particle acidity. *Atmospheric Chemistry and Physics*, 21(19), 14983-15001, <https://doi.org/10.5194/acp-21-14983-2021>, 2021.
- Kerkweg, A., Buchholz, J., Ganzeveld, L., Pozzer, A., Tost, H., and Jöckel, P.: An implementation of the dry removal processes DRY DEPosition and SEDimentation in the Modular Earth Submodel System (MESSy). *Atmospheric Chemistry and Physics*, 6(12), 4617-4632, <https://doi.org/10.5194/acp-6-4617-2006>, 2006.
- Kim, Y. P., Seinfeld, J. H., and Saxena, P.: Atmospheric gas-aerosol equilibrium I. Thermodynamic model. *Aerosol Science and Technology*, 19(2), 157-181, <https://doi.org/10.1080/02786829308959628>, 1993.
- Klingmüller, K., Metzger, S., Abdelkader, M., Karydis, V. A., Stenchikov, G. L., Pozzer, A., and Lelieveld, J.: Revised mineral dust emissions in the atmospheric chemistry-climate model EMAC (MESSy 2.52 DU_Astitha1 KKDU2017 patch). *Geoscientific Model Development*, 11(3), 989-1008, <https://doi.org/10.5194/gmd-11-989-2018>, 2018.
- Klingmüller, K., Lelieveld, J., Karydis, V. A., and Stenchikov, G. L.: Direct radiative effect of dust-pollution interactions. *Atmospheric chemistry and physics*, 19(11), 7397-7408, <https://doi.org/10.5194/acp-19-7397-2019>, 2019.
- Klingmüller, K., Karydis, V. A., Bacer, S., Stenchikov, G. L., and Lelieveld, J.: Weaker cooling by aerosols due to dust-pollution interactions. *Atmospheric Chemistry and Physics*, 20(23), 15285-15295, <https://doi.org/10.5194/acp-20-15285-2020>, 2020.
- Kusik, C. L. and HP, M.: 1978-Meissner H.P.: Electrolyte Activity Coefficients in Inorganic Processing. AIChE Symp. Series, 173, 14-20, 1978.
- Lelieveld, J., Evans, J. S., Fnais, M., Giannadaki, D., and Pozzer, A.: The contribution of outdoor air pollution sources to premature mortality on a global scale. *Nature*, 525(7569), 367-371, <https://doi.org/10.1038/nature15371>, 2015.

- Lohmann, U. and Ferrachat, S.: Impact of parametric uncertainties on the present-day climate and on the anthropogenic aerosol effect. *Atmospheric Chemistry and Physics*, 10(23), 11373-11383, <https://doi.org/10.5194/acp-10-11373-2010>, 2010.
- Manisalidis, I., Stavropoulou, E., Stavropoulos, A., and Bezirtzoglou, E.: Environmental and health impacts of air pollution: a review. *Frontiers in public health*, 14, <https://doi.org/10.3389/fpubh.2020.00014>, 2020.
- Marais, E. A., Jacob, D. J., Jimenez, J. L., Campuzano-Jost, P., Day, D. A. and co-authors: Aqueous-phase mechanism for secondary organic aerosol formation from isoprene: application to the southeast United States and co-benefit of SO₂ emission controls. *Atmospheric Chemistry and Physics*, 16(3), 1603-1618, <https://doi.org/10.5194/acp-16-1603-2016>, 2016.
- Meissner, H. P. and Peppas, N. A.: Activity coefficients – aqueous solutions of polybasic acids and their salts, *AIChE Journal*, 19(4), 806–809, <https://doi.org/10.1002/aic.690190419>, 1973.
- Metzger, S., Dentener, F., Pandis, S., and Lelieveld, J., *Gas/aerosol partitioning, 1, A computationally efficient model, *Journal of Geophysical Research: Atmospheres*, 107(D16), <https://doi.org/10.1029/2001JD001102>, 2002.*
- Miinalainen, T., Kokkola, H., Lehtinen, K. E., and Kühn, T.: Comparing the radiative forcings of the anthropogenic aerosol emissions from Chile and Mexico. *Journal of Geophysical Research: Atmospheres*, 126(10), <https://doi.org/10.1029/2020JD033364>, 2021.
- Myhre, G., Samset, B. H., Schulz, M., Balkanski, Y., Bauer, S., Berntsen, T. K. and co-authors: Radiative forcing of the direct aerosol effect from AeroCom Phase II simulations. *Atmospheric Chemistry and Physics*, 13(4), 1853-1877, <https://doi.org/10.5194/acp-13-1853-2013>, 2013.
- Nenes, A., Pandis, S. N., and Pilinis, C.: ISORROPIA: A new thermodynamic equilibrium model for multiphase multicomponent inorganic aerosols. *Aquatic geochemistry*, 4, 123-152, <https://doi.org/10.1023/A:1009604003981>, 1998.
- Nenes, A., Pandis, S. N., Weber, R. J., and Russell, A.: Aerosol pH and liquid water content determine when particulate matter is sensitive to ammonia and nitrate availability. *Atmospheric Chemistry and Physics*, 20(5), 3249-3258, <https://doi.org/10.5194/acp-20-3249-2020>, 2020.
- Pilinis, C. and Seinfeld, J. H.: Continued development of a general equilibrium model for inorganic multicomponent atmospheric aerosols. *Atmospheric Environment (1967)*, 21(11), 2453-2466, [https://doi.org/10.1016/0004-6981\(87\)90380-5](https://doi.org/10.1016/0004-6981(87)90380-5), 1987.
- Pope, C. A., Burnett, R. T., Turner, M. C., Cohen, A., Krewski, D. and co-authors: Lung cancer and cardiovascular disease mortality associated with ambient air pollution and cigarette smoke: shape of the exposure–response relationships. *Environmental health perspectives*, 119(11), 1616-1621, <https://doi.org/10.1289/ehp.1103639>, 2011.
- Pozzer, A., Jöckel, P., Sander, R., Williams, J., Ganzeveld, L., and Lelieveld, J.: The MESSy-submodel AIRSEA calculating the air-sea exchange of chemical species. *Atmospheric Chemistry and Physics*, 6(12), 5435-5444, <https://doi.org/10.5194/acp-6-5435-2006>, 2006.
- Pringle, K. J., Tost, H., Message, S., Steil, B., Giannadaki, D. and co-authors: Description and evaluation of GMXe: a new aerosol submodel for global simulations (v1). *Geoscientific Model Development*, 3(2), 391-412, <https://doi.org/10.5194/gmd-3-391-2010>, 2010.
- Pringle, K. J., Tost, H., Message, S., Steil, B., Giannadaki, D. and co-authors: Corrigendum to “Description and evaluation of GMXe: a new aerosol submodel for global simulations (v1)”. *Geoscientific Model Development*, 3(2), 413-413, <https://doi.org/10.5194/gmd-3-413-2010>, 2010.
- Putaud, J. P., Van Dingenen, R., Alastuey, A., Bauer, H., Birmili, W. and co-authors: A European aerosol phenomenology–3: Physical and chemical characteristics of particulate matter from 60 rural, urban, and kerbside sites across Europe. *Atmospheric Environment*, 44(10), 1308-1320, <https://doi.org/10.1016/j.atmosenv.2009.12.011>, 2010.

- Roeckner, E., Brokopf, R., Esch, M., Giorgetta, M., Hagemann, S. and co-authors: Sensitivity of simulated climate to horizontal and vertical resolution in the ECHAM5 atmosphere model. *Journal of Climate*, 19(16), 3771-3791, <https://doi.org/10.1175/JCLI3824.1>, 2006.
- Saiz-Lopez, A. and von Glasow, R.: Reactive halogen chemistry in the troposphere. *Chemical Society Reviews*, 41(19), 6448-6472, <https://doi.org/10.1039/C2CS35208G>, 2012.
- Sander, R., Baumgaertner, A., Cabrera-Perez, D., Frank, F., Gromov, S. and co-authors: The community atmospheric chemistry box model CAABA/MECCA-4.0. *Geoscientific model development*, 12(4), 1365-1385, <https://doi.org/10.5194/gmd-12-1365-2019>, 2019.
- Savoie, D. L. and Prospero, J.: Particle size distribution of nitrate and sulfate in the marine atmosphere. *Geophysical Research Letters*, 9(10), 1207-1210, <https://doi.org/10.1029/GL009i010p01207>, 1982.
- Saxena, P., Hudischewskyj, A. B., Seigneur, C., and Seinfeld, J. H.: A comparative study of equilibrium approaches to the chemical characterization of secondary aerosols. *Atmospheric Environment* (1967), 20(7), 1471-1483, [https://doi.org/10.1016/0004-6981\(86\)90019-3](https://doi.org/10.1016/0004-6981(86)90019-3), 1986.
- Seinfeld, J. H. and Pandis, S. N.: *Atmospheric chemistry and physics: from air pollution to climate change*. John Wiley & Sons, ISBN 1118947401, 2016.
- Silva, P. J., Vawdrey, E. L., Corbett, M., and Erupe, M.: Fine particle concentrations and composition during wintertime inversions in Logan, Utah, USA. *Atmospheric Environment*, 41(26), 5410-5422, <https://doi.org/10.1016/j.atmosenv.2007.02.016>, 2007.
- Song, S., Gao, M., Xu, W., Shao, J., Shi, G., Wang, S. and co-authors: Fine-particle pH for Beijing winter haze as inferred from different thermodynamic equilibrium models. *Atmospheric Chemistry and Physics*, 18(10), 7423-7438, <https://doi.org/10.5194/acp-18-7423-2018>, 2018.
- Szopa, S., Naik, V., Adhikary, B., Artaxo, P., Berntsen, T. and co-authors. 2021. Short-lived climate forcers, AGU Fall Meeting 2021, held in New Orleans, LA, 13-17 December 2021, id. U13B-06, 2021AGUFM.U13B.06S, 2021.
- Tang, Y. S., Flechard, C. R., Dammgen, U., Vidic, S., Djuricic, V. and co-authors: Pan-European rural monitoring network shows dominance of NH₃ gas and NH₄NO₃ aerosol in inorganic atmospheric pollution load. *Atmospheric Chemistry and Physics*, 21(2), 875-914, <https://doi.org/10.5194/acp-21-875-2021>, 2021.
- ~~Tarin~~ Tarin-Carrasco, P., Im, U., Geels, C., Palacios-Peña, L., and Jiménez-Guerrero, P.: Contribution of fine particulate matter to present and future premature mortality over Europe: A non-linear response. *Environment international*, 153, 106517, <https://doi.org/10.1016/j.envint.2021.106517>, 2021.
- The Acid Deposition Monitoring Network in East Asia, available at : <https://monitoring.eanet.asia/document/public/index>
- Tost, H., Jöckel, P., Kerkweg, A., Sander, R., and Lelieveld, J.: A new comprehensive SCAVenging submodel for global atmospheric chemistry modelling. *Atmospheric Chemistry and Physics*, 6(3), 565-574, <https://doi.org/10.5194/acp-6-565-2006>, 2006.
- Tost, H., Jöckel, P., Kerkweg, A., Pozzer, A., Sander, R., and Lelieveld, J.: Global cloud and precipitation chemistry and wet deposition: tropospheric model simulations with ECHAM5/MESy1. *Atmospheric Chemistry and Physics*, 7(10), 2733-2757, <https://doi.org/10.5194/acp-7-2733-2007>, 2007.
- Tsimpidi, A. P., Karydis, V. A., and Pandis, S. N.: [Response of Inorganic Fine Particulate Matter to Emission Changes of Sulfur Dioxide and Ammonia: The Eastern United States as a Case Study](https://doi.org/10.3155/1047-3289.57.12.1489), *Journal of the Air & Waste Management Association*, 57(12), 1489-1498, <https://doi.org/10.3155/1047-3289.57.12.1489>, 2007.

Tsimpidi, A. P., Karydis, V. A., Pozzer, A., Pandis, S. N., and Lelieveld, J.: ORACLE (v1. 0): module to simulate the organic aerosol composition and evolution in the atmosphere. *Geoscientific Model Development*, 7(6), 3153-3172, <https://doi.org/10.5194/gmd-7-3153-2014>, 2014.

Tsimpidi, A. P., Karydis, V. A., Pozzer, A., Pandis, S. N., and Lelieveld, J.: ~~Global combustion sources~~ ORACLE 2-D (v2.0): an efficient module to compute the volatility and oxygen content of organic aerosols: aerosol with a global chemistry-climate model-comparison with 84 AMS factor analysis data sets. *Atmospheric Chemistry and Physics*, 16(14), 8939-8962, *Geoscientific Model Development*, 11(8), 3369-3389, <https://doi.org/10.5194/acp-16-8939-2016>, 2016 <https://doi.org/10.5194/gmd-11-3369-2018>, 2018.

U.S. Environmental Protection Agency Clean Air Markets Division *Clean Air Status and Trends Network (CASTNET)*, available at : <https://www.epa.gov/castnet>

van der Werf, G. R., Randerson, J. T., Giglio, L., Collatz, G. J., Mu, M. and co-authors: Global fire emissions and the contribution of deforestation, savanna, forest, agricultural, and peat fires (1997–2009). *Atmospheric chemistry and physics*, 10(23), 11707-11735, <https://doi.org/10.5194/acp-10-11707-2010>, 2010.

Vignati, E., Wilson, J., and Stier, P.: M7: An efficient size-resolved aerosol microphysics module for large-scale aerosol transport models. *Journal of Geophysical Research: Atmospheres*, 109(D22), <https://doi.org/10.1029/2003JD004485>, 2004.

Weagle, C. L., Snider, G., Li, C., Van Donkelaar, A., Philip, S., Bissonnette, P., Burke, J., Jackson, J., Latimer, R., and Stone, E.: Global sources of fine particulate matter: interpretation of PM_{2.5} chemical composition observed by SPARTAN using a global chemical transport model, *Environmental science & technology*, 52(20), 11670-11681, <https://doi.org/10.1021/acs.est.8b01658>, 2018.

Wexler, A. S. and Clegg, S. L.: Atmospheric aerosol models for systems including the ions H⁺, NH₄⁺, Na⁺, SO₄²⁻, NO₃⁻, Cl⁻, Br⁻, and H₂O. *Journal of Geophysical Research: Atmospheres*, 107(D14), ACH-14, <https://doi.org/10.1029/2001JD000451>, 2002.

Wexler, A. S. and Seinfeld, J. H.: Second-generation inorganic aerosol model. *Atmospheric Environment. Part A. General Topics*, 25(12), 2731-2748, [https://doi.org/10.1016/0960-1686\(91\)90203-J](https://doi.org/10.1016/0960-1686(91)90203-J), 1991.

Wolff, G. T.: On the nature of nitrate in coarse continental aerosols. *Atmospheric Environment (1967)*, 18(5), 977-981, [https://doi.org/10.1016/0004-6981\(84\)90073-8](https://doi.org/10.1016/0004-6981(84)90073-8), 1984.

World Health Organization. Ambient (outdoor) air pollution: [https://www.who.int/news-room/fact-sheets/detail/ambient-\(outdoor\)-air-quality-and-health](https://www.who.int/news-room/fact-sheets/detail/ambient-(outdoor)-air-quality-and-health), last access: 19 December 2022.

Xu, G., Zhang, Q., Yao, Y., and Zhang, X.: Changes in PM_{2.5} sensitivity to NO_x and NH₃ emissions due to a large decrease in SO₂ emissions from 2013 to 2018. *Atmospheric and Oceanic Science Letters*, 13(3), 210-215, <https://doi.org/10.1080/16742834.2020.1738009>, 2020.

Yan, W., Toppoff, M., Rose, C., and Gmehling, J.: Prediction of vapor-liquid equilibria in mixed-solvent electrolyte systems using the group contribution concept. *Fluid Phase Equilibria*, 162(1-2), 97-113, [https://doi.org/10.1016/S0378-3812\(99\)00201-0](https://doi.org/10.1016/S0378-3812(99)00201-0), 1999.

Yienger, J. J. and Levy, H.: Empirical model of global soil-biogenic ~~NO_x~~NO_x emissions. *Journal of Geophysical Research: Atmospheres*, 100(D6), 11447-11464, <https://doi.org/10.1029/95JD00370>, 1995.

Zakoura, M. and Pandis, S. N.: Overprediction of aerosol nitrate by chemical transport models: The role of grid resolution. *Atmospheric Environment*, 187, 390-400, <https://doi.org/10.1016/j.atmosenv.2018.05.066>, 2018.

Zuend, A., Marcolli, C., Luo, B. P., and Peter, T.: A thermodynamic model of mixed organic-inorganic aerosols to predict activity coefficients. *Atmospheric Chemistry and Physics*, 8(16), 4559-4593, <https://doi.org/10.5194/acp-8-4559-2008>, 2008.

Zuend, A., Marcolli, C., Booth, A. M., Lienhard, D. M., Soonsin, V., Krieger, U. K., Topping, D. O., McFiggans, G., Peter, T., and Seinfeld, J. H.: New and extended parameterization of the thermodynamic model

Formatted: Font: (Default) Calibri, 11 pt, Font color: Auto, Pattern: Clear

AIOMFAC: calculation of activity coefficients for organic-inorganic mixtures containing carboxyl, hydroxyl, carbonyl, ether, ester, alkenyl, alkyl, and aromatic functional groups, *Atmospheric Chemistry and Physics*, 11(17), 9155-9206, <https://doi.org/10.5194/acp-11-9155-2011>, 2011.

Tsimpidi, A. P., Karydis, V. A., and Pandis, S. N.: Response of Inorganic Fine Particulate Matter to Emission Changes of Sulfur Dioxide and Ammonia: The Eastern United States as a Case Study, *Journal of the Air & Waste Management Association*, 57, 1489–1498, 10.3155/1047-3289.57.12.1489, 2007.

Tsimpidi, A. P., Karydis, V. A., Pozzer, A., Pandis, S. N., and Lelieveld, J.: ORACLE (v1.0): module to simulate the organic aerosol composition and evolution in the atmosphere, *Geosci. Model Dev.*, 7, 3153–3172, 10.5194/gmd-7-3153-2014, 2014.

Tsimpidi, A. P., Karydis, V. A., Pozzer, A., Pandis, S. N., and Lelieveld, J.: ORACLE 2-D (v2.0): an efficient module to compute the volatility and oxygen content of organic aerosol with a global chemistry-climate model, *Geosci. Model Dev.*, 11, 3369–3389, 10.5194/gmd-11-3369-2018, 2018.

Formatted: Indent: Left: 0 cm, Hanging: 1.27 cm, Line spacing: single